



## NUMERICAL MODELLING OF LAHENDONG GEOTHERMAL SYSTEM, INDONESIA

**Ahmad Yani**

Pertamina - Area Geothermal Lahendong  
Jl. Raya Tomohon No. 420  
Tomohon 95362  
INDONESIA  
*ahmadyani@pertamina.com*

### ABSTRACT

Lahendong geothermal field is one of the most promising geothermal areas in Indonesia. The first 20 MWe Unit started production in June 2001 and is supplied by about 40 kg/s of two-phase geothermal fluid. Today, the power plant is being developed for two additional 20 MWe units, II and III, that are scheduled to be commissioned in 2007 and 2008. This paper describes the development of a detailed numerical reservoir model of the geothermal system underlying the Lahendong geothermal area. The purpose of this study is to review the reservoir engineering aspects of the field and develop a numerical model, based on pressure and temperature data and well output. The TOUGH2 simulator was employed and coupled with interface software developed by Pertamina. Temperature and pressure profiles in the Lahendong geothermal field were studied and their interpretation supports the existing conceptual model of the Lahendong geothermal reservoir. The numerical model was used to calculate a future forecast production of 60 MWe to the year 2036, resulting in a 10 bar reservoir pressure drawdown. The forecast results are, however, uncertain due to a lack of pressure drawdown data, which are essential for model calibration.

### 1. INTRODUCTION

The Lahendong geothermal field is located in the Minahasa of the north arm of Sulawesi, one of the major geothermal resources in Indonesia, and about 40 km from Manado city, North Sulawesi (Figure 1). This area is characterized by active volcanoes that form the volcanic inner arc of Minahasa, which is highly active tectonically.

The high-temperature geothermal systems in this area are divided into two different categories based on reservoir temperatures, those with very high temperatures ( $350^{\circ}\text{C}$ ) in the south and those with more modest temperatures in the north ( $250^{\circ}\text{C}$ ). From 1986 to 2006, 23 wells were drilled from eight drilling pads. The first geothermal power plant in Lahendong, Unit I, which produces 20 MWe, was commissioned in 2001, and has been operating steadily since. The production of 20 MWe is supplied by 40 kg/s of steam from four production wells. The two-phase fluid produced from these wells is transported to the separator station about 500 m northwest of the drilling pad. The condensate and

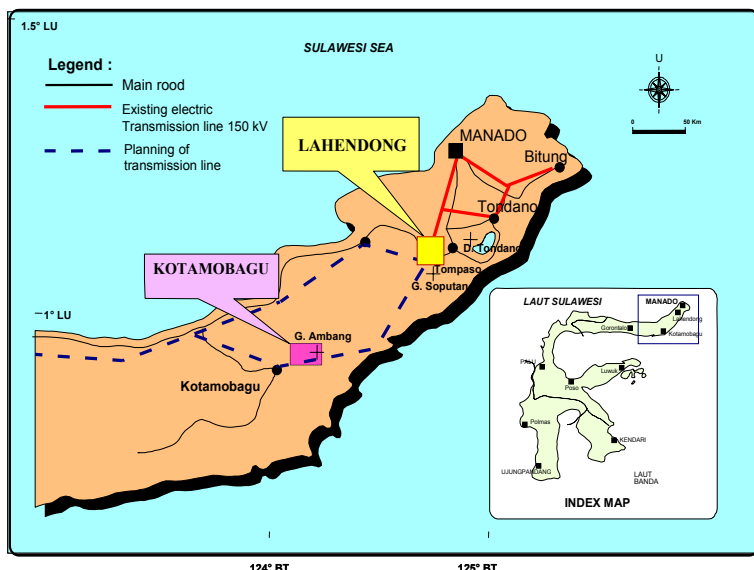


FIGURE 1: Location map of Lahendong geothermal field

tectonic and volcanic study in Minahasa of the north arm of Sulawesi related to the Lahendong geothermal field are summarised by Siahaan et al. (2005).

The last resource study in this area was done by PT. PLN (Persero) in 2005. A TOUGH2 numerical model was applied in the study. The study included geological, geophysical, geochemical and reservoir engineering studies based on the technical data and reports prepared by PT. PERTAMINA (Persero).

This study is a student paper of the United Nation University Geothermal Training Programme (UNU-GTP) in Iceland and a final project report for completion of the training programme. The paper describes a 3-dimensional numerical simulation model of the Lahendong geothermal field, where the TOUGH2 simulator was coupled with a user interface. Available data from the Lahendong field was reviewed and analysed in light of existing conceptual models of the field, which were used as a foundation for the numerical model developed and described here. Different boundary conditions were applied than in the last modelling study of PT. PLN (2005). The data that this project is based on is mostly internal data from Pertamina (Marihot et al., 2004a, 2004b, 2005a, 2005b, 2005c, 2005d, 2006; Sujata, 2006; Yani, 2006 and other production monitoring data from 2006). The natural state of numerical modelling is compared with observed pressure and temperature data from the wells in the field. Due to limited time for this project, the final result of the study is a future forecast calculation that evaluates reservoir performance in a 36 year production time frame if the power production is increased from 20 to 60 MWe.

## 2. THE LAHENDONG GEOTHERMAL FIELD

### 2.1 Geology and tectonic information

The Lahendong geothermal field is characterized by active volcanoes that form the volcanic inner arc of Minahasa, consisting of Mt. Soputan, Mt. Lokon-Empung, Mt. Mahawu and Mt. Klabat, and Mt. Dua Saudara, trending southwest to northeast. Structurally, the area comprises some fault patterns which are major strike-slip faults trending NE-SW, NW-SE and normal faults trending N-S (Figure 2). The most intensively faulted area is west of Pangalombian caldera (around Lake Linau). The active strike slip left lateral fault, trending NE-SW, is located on the crest of a volcanic inner arc of Minahasa, aligning from Mt. Soputan on the south-west side to Mt. Klabat on the northeast side.

brine water is injected back into the reservoir through one injection well, east of the main field. A further development of 40 MWe is now underway. New units are scheduled to be commissioned in 2007 (Unit II with 20 MWe) and in 2008 (Unit III also with 20 MWe).

There are many published reports concerned with resource studies on Lahendong geothermal field. Geological mapping of Lahendong and Tompaso was done by Ganda and Sunaryo, the interpretation of aerial photos by D. Robert, and the interpretation of Landsat and aerial photos was carried out by Siahaan. These studies and an additional

This fault controls the development of Tondano and Pangolombian calderas and separates the geo-thermal system of the Lahendong field and the Tompaso prospect (Figure 2). The eastern rim of the Tondano caldera can be delineated where the western and southern rims were covered by the lava product of Mt. Lengkoan, Mt. Sempu and Soputan (Siahaan et al., 2005)

The main predicted faults are shown on the geological map on Figure 3, from previous aerial photo analysis and geophysical exploration. The faults F1 and F2, trending NW-SE, dip toward southwest, faults F3, F4, F5 and F10, trending N-S, dip towards west, while faults F6, F7, F8 and F11, trending NE-SW, dip towards southeast. A major lost circulation zone is recognized around faults F0, F1, F2, F7, F8 and F11 in most of the drilled wells. Fault F0, trending NW-SE and dipping towards northeast, was predicted by the latest model from PERTAMINA to explain the feed point of well LHD-11 (PT. PLN, 2005).

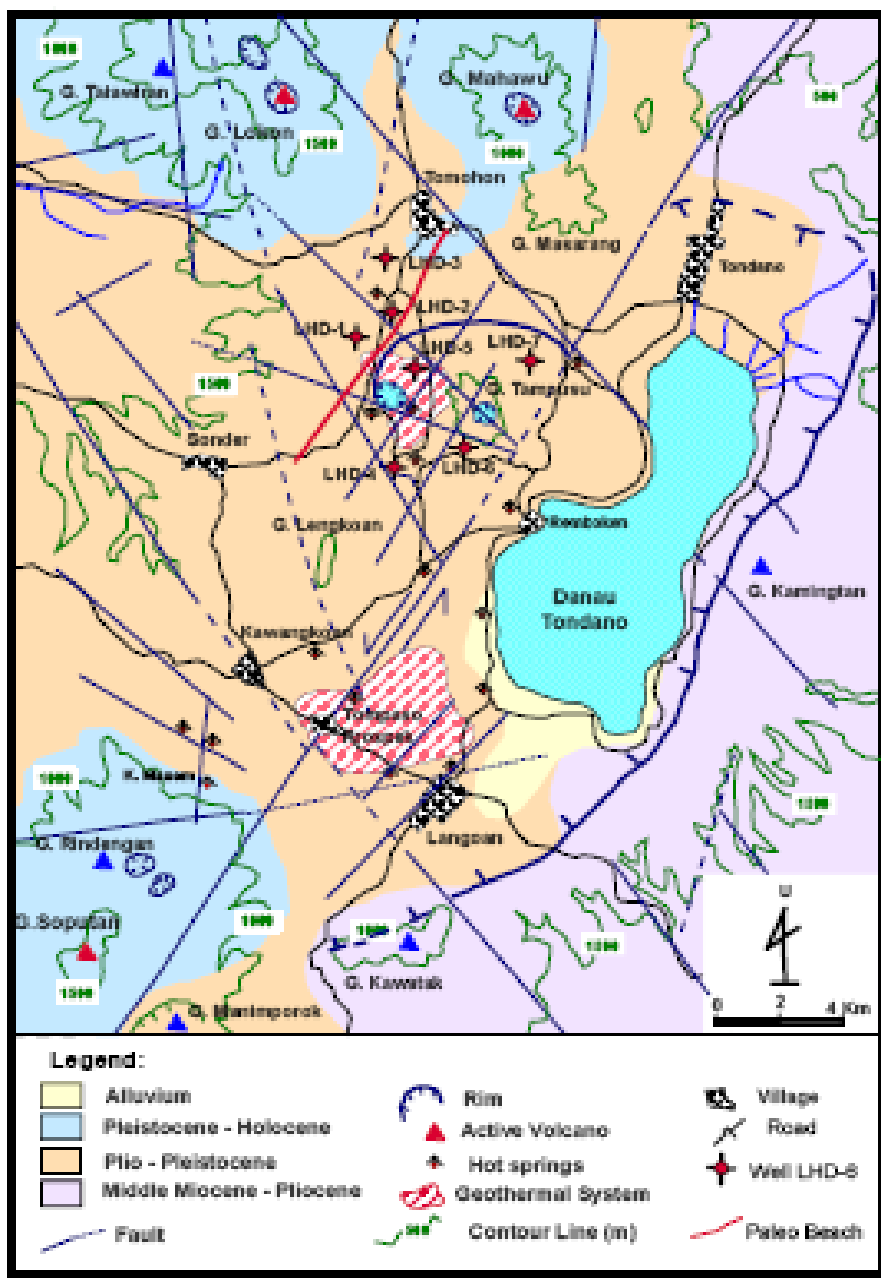


FIGURE 2: The geological map and fault pattern in the Minahasa compartment (Siahaan et al., 2005)

The volcano-stratigraphy of the Lahendong geothermal field can be divided into three main rock units, the Pre-Tondano unit, the Syn-Tondano unit and the Post Tondano unit. Moreover, the Post-Tondano unit is divided into two volcanic products by the Pre-Caldera and Post-Caldera activity of the Pangolombian caldera,. The Pre-caldera volcanic products consist of the Pangolombian formation and Lengkoan formation, while the Post-caldera volcanic products consist of the Kasuratan formation, Tampusu formation, Kasuan formation, Linau formation and the Masarang formation. As shown in Figure 3, volcanic rocks cover the Lahendong geothermal field and its surrounding area.

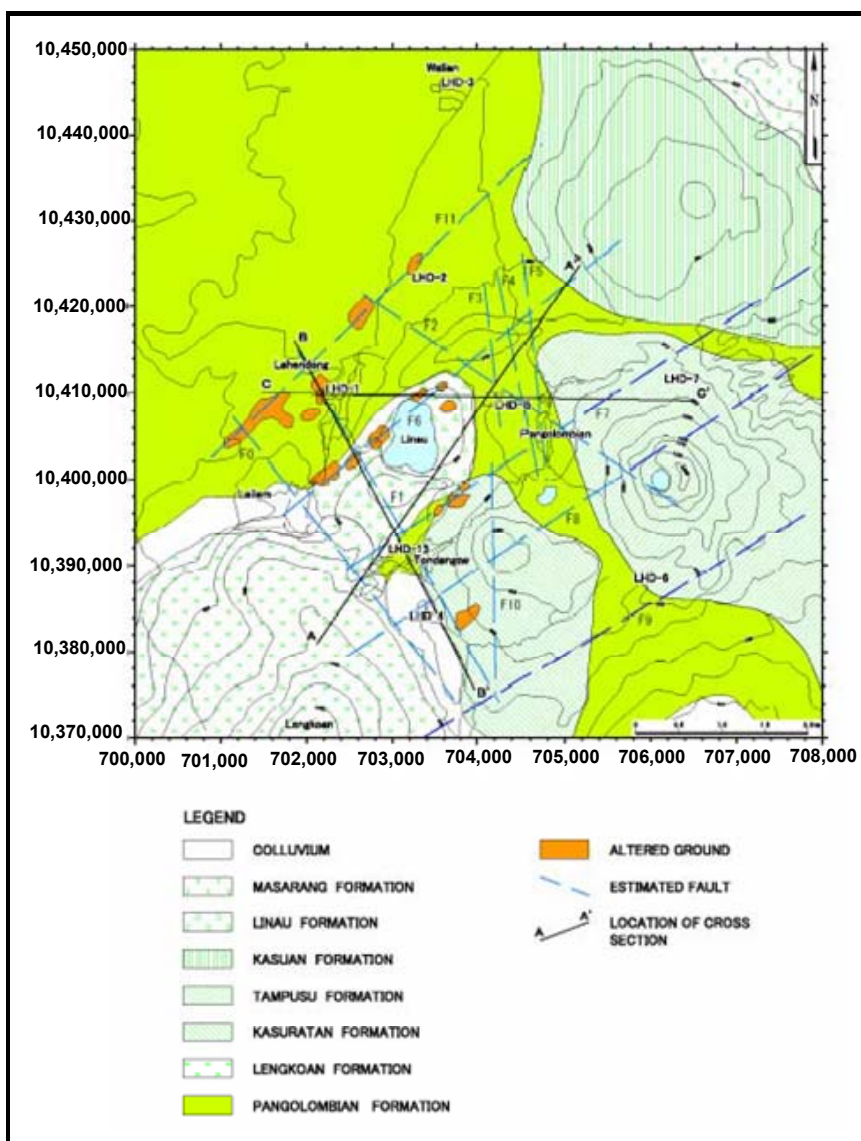


FIGURE 3: Geological map of Lahendong (PT. PLN 2005)

field and they are distributed in two different areas, the north block and the south block (Figure 5). Wells in the south block (pads LHD-13 and 4) range in temperature between 300 and 350°C with pressures around 250 bar-g. Wells in the north block (pad LHD-5) have lower temperatures, ranging from 200 to 250°C with pressures about 150 bar-g. The distribution of subsurface pressure and temperature in the Lahendong geothermal system is shown in Figure 6. From the pressure and temperature distributions (Figure 5), the temperature profiles of the wells can be classified into difference types (Figure 7):

- Well LHD-01 shows indications of lateral hot water flow near the surface, around 500 m a.s.l. The deeper part indicates a heat conductive flow profile;
- Wells LHD-02 and LHD-3 indicate conductive flow temperature profiles with maximum temperatures of 190 and 280°C;
- Wells in pad LHD-13 (LHD-13, 14, 16, 17 and 18) show conduction flow temperature profiles in the upper part, where the temperature increases linearly with depth, but well LHD-13 shows clear signs of a convection system at 1500 m b.s.l. where temperature exceeds 300°C;
- Well LHD-17 also shows temperatures above 300°C at 500 m b.s.l., which is 1000 m shallower than in LHD-13;

The Pre-Tondano unit does not crop out in the Lahendong field, although data from deep wells show that this unit is distributed widely under sea level (Figure 4). From drilling data, products from hydrothermal alteration are mainly recognized on the northeast side of Lake Linau. Their mineralogy is characterized by kaolinite. This indicates that hydrothermal alteration near the surface resulted mainly from acidic hot water. As shown in Figure 3, most of altered grounds are distributed along the faults F1, F6, F7 and F11. This is used as an indication that hydrothermal activity of acidic hot water near the surface is controlled by these faults (Siahaan et al., 2005; PT. PLN, 2005).

## 2.2 Temperature and pressure

To date, 23 wells have been drilled in the Lahendong geothermal

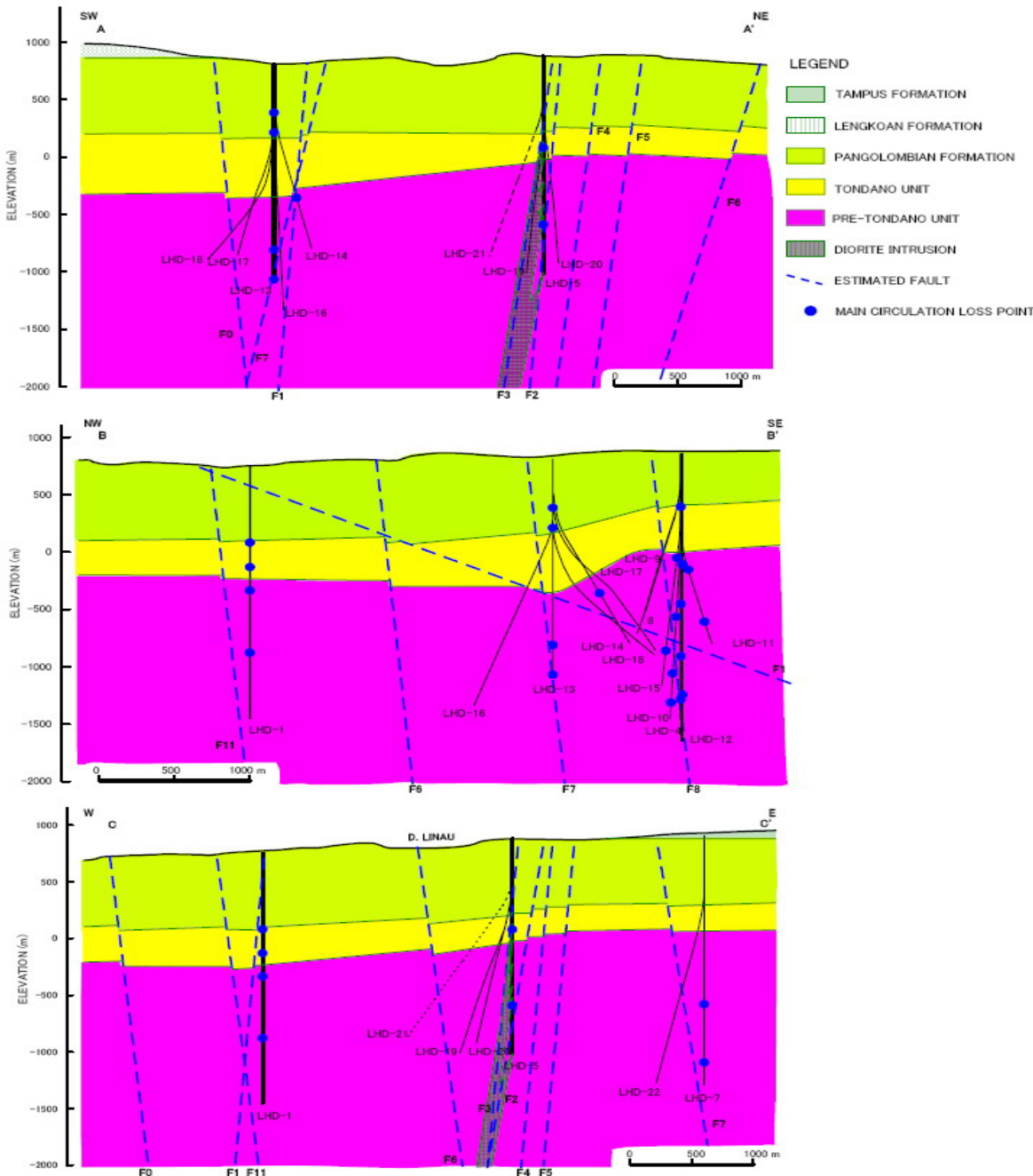


FIGURE 4: Geological cross-sections through the Lahendong field,  
locations are shown on Figure 3 (PT. PLN, 2005)

- Wells in pad LHD-4 (LHD-4, 11 and 12) are affected by lateral cold water flow at sea level depth, but below sea level the temperature profiles bear witness to a convective geothermal system with a temperature of about 320°C and maximum temperature of about 350°C.
  - Temperature profiles measured in wells in pad LHD-5 (LHD-5, 19, 20, 21 and 23) have heat conduction characteristics with lateral hot water flow at around 500 m a.s.l. The maximum borehole temperature measured in these wells is about 153°C.
  - Well LHD-6, which is of a heat conductive type, shows lateral flow of cold water at depths around 500 m a.s.l.
  - Injection wells at pad LHD-7 (LHD-7 and 22) have the lowest temperature in the field with a maximum temperature of 110°C; the temperature profiles indicate a down-flow of cold water in this part of the geothermal field.

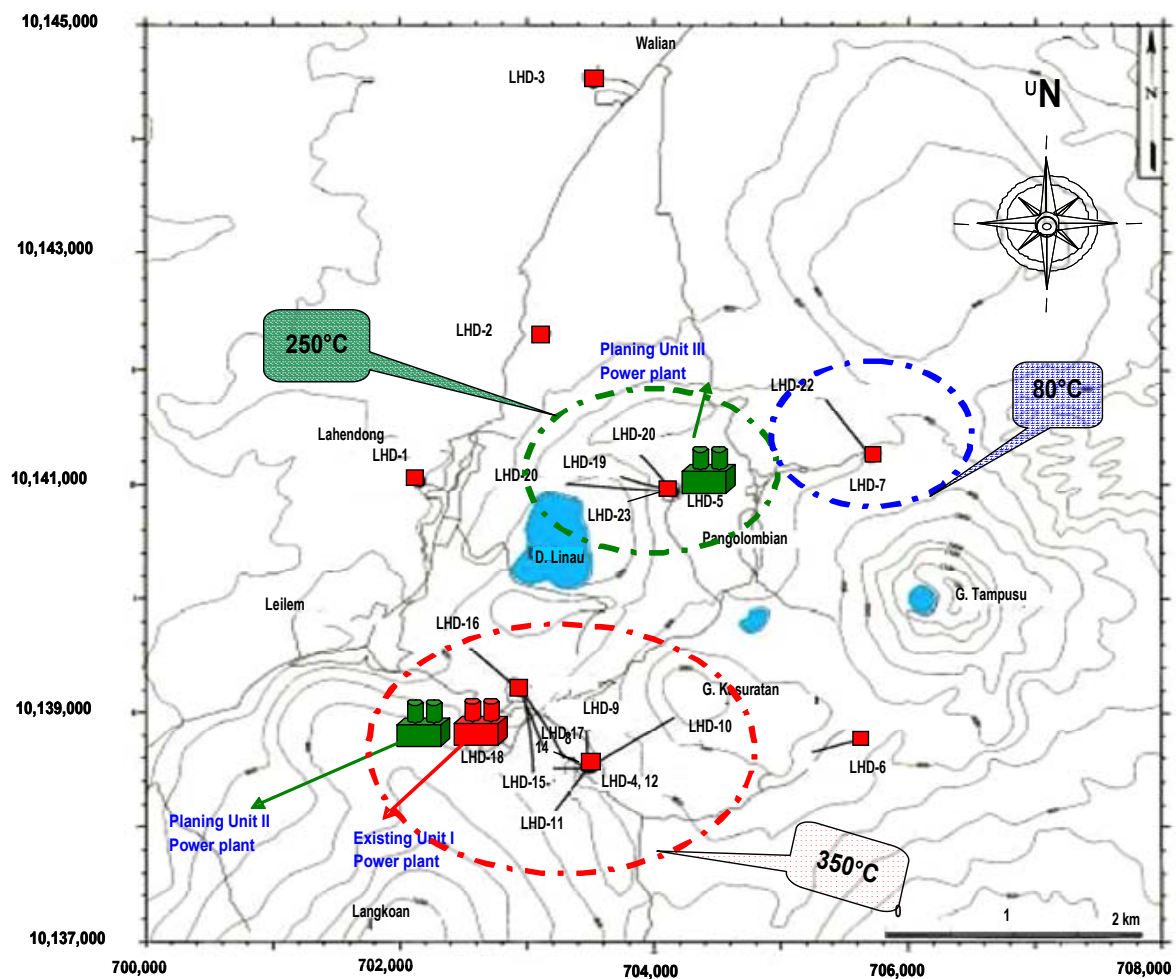


FIGURE 5: Locations of wells in the Lahendong geothermal field

Based on the temperature profiles described above, it is considered that the heat source of the reservoir is around wells in pads LHD-4 and LHD-13. Temperature profiles from wells LHD-2, 3, 6, 7, and 22 show thermal gradient rock temperatures which are generally found outside the main reservoir area. Another heat source is considered to be close to well LHD-1 in the northern part of the field. Even though it has low temperature close to the surface, the temperature at 1000 m b.s.l. is close to 300°C. This was confirmed through chemical study and analysis in the area (PT. PLN, 2005).

### 2.3 Structures and permeability

From the geological analysis, previous aerial photo analysis and geophysical exploration study, it is estimated that there are 12 fault systems controlling this field (Figure 3, PT. PLN, 2005). Fluid mobility in this area is controlled by fracture permeability. Distribution of circulation loss points of each drilled well is correlated with estimated fault location, as given in Figure 8. For simplicity's sake, the locations of circulation loss zones were classified into three interval zones. The intervals are: from sea level to 500 m b.s.l., from 500 to 1000 m b.s.l. and from 1000 m b.s.l. to the total depth of each well. Most of the circulation loss zones are located close to the intersection of faults F1 and F8.

Rock permeability is the most important parameter controlling the discharge capacity of geothermal wells. Well completion tests were always performed at the end of drilling in order to estimate the formation permeability around the wells. The tests were usually water injection tests where borehole pressure is monitored while water is injected into the well at various rates. The fall-off pressure was

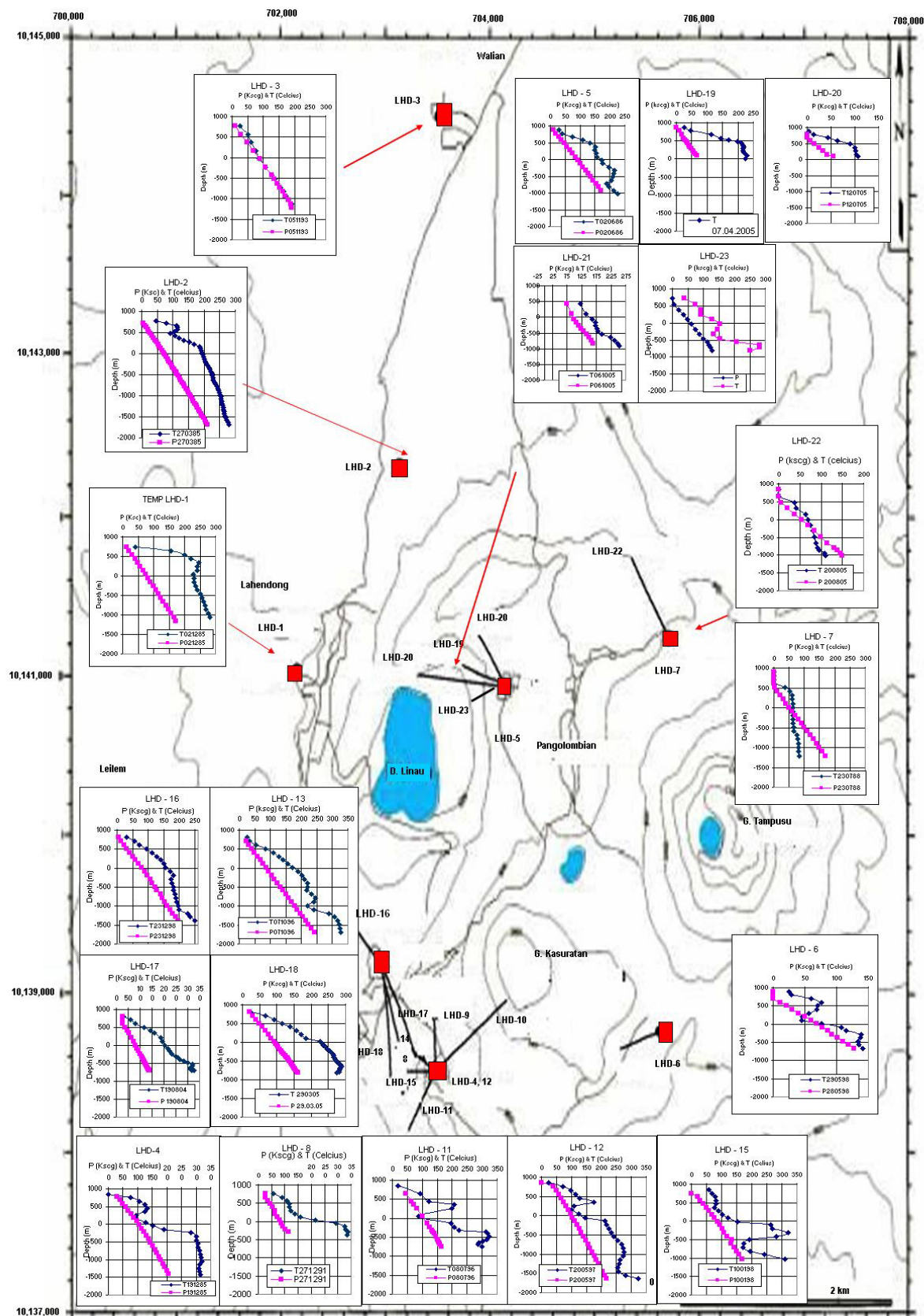


FIGURE 6: Pressure and temperature profiles in the Lahendong geothermal field

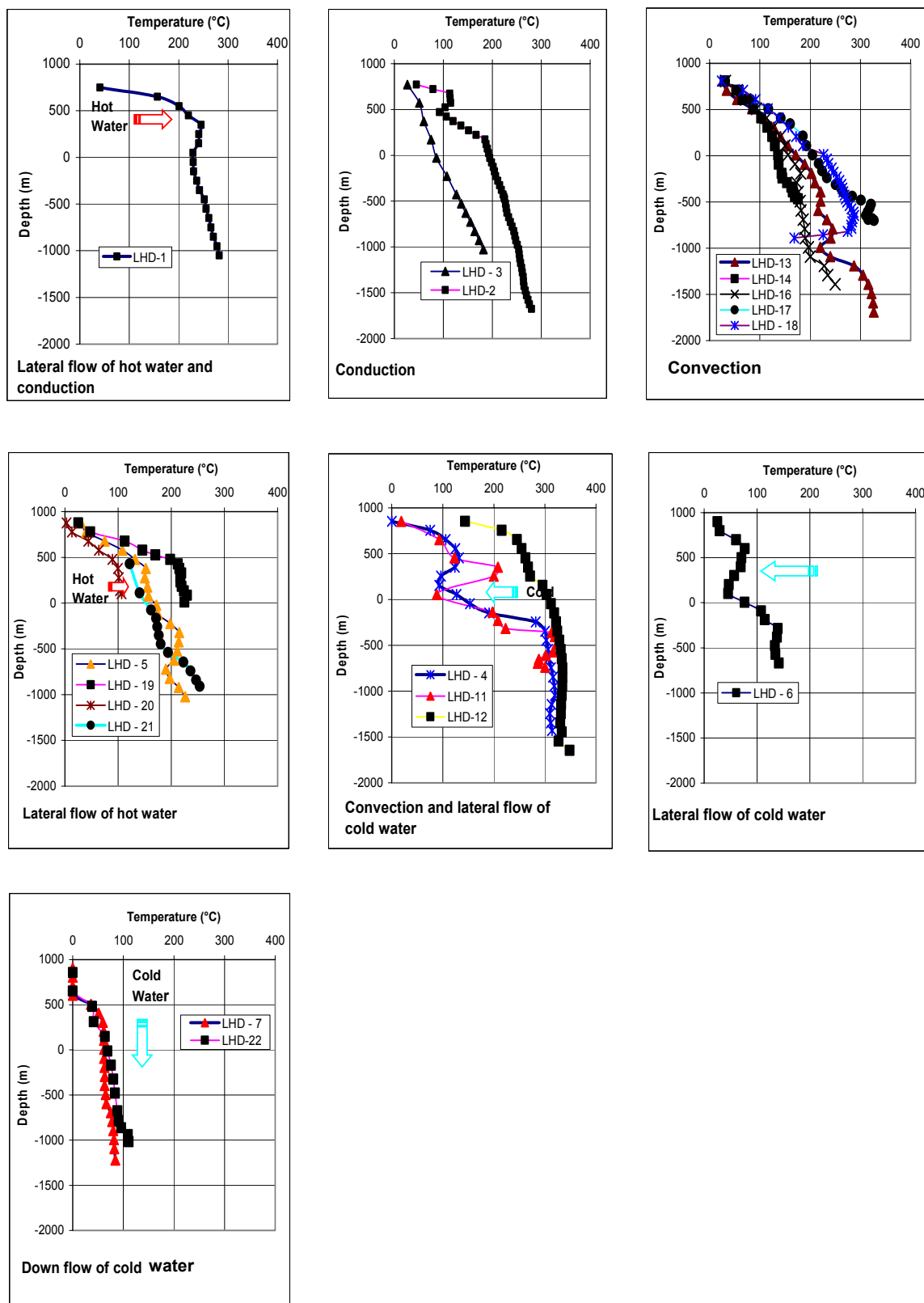


FIGURE 7: Classification of well temperature profiles in the Lahendong field.

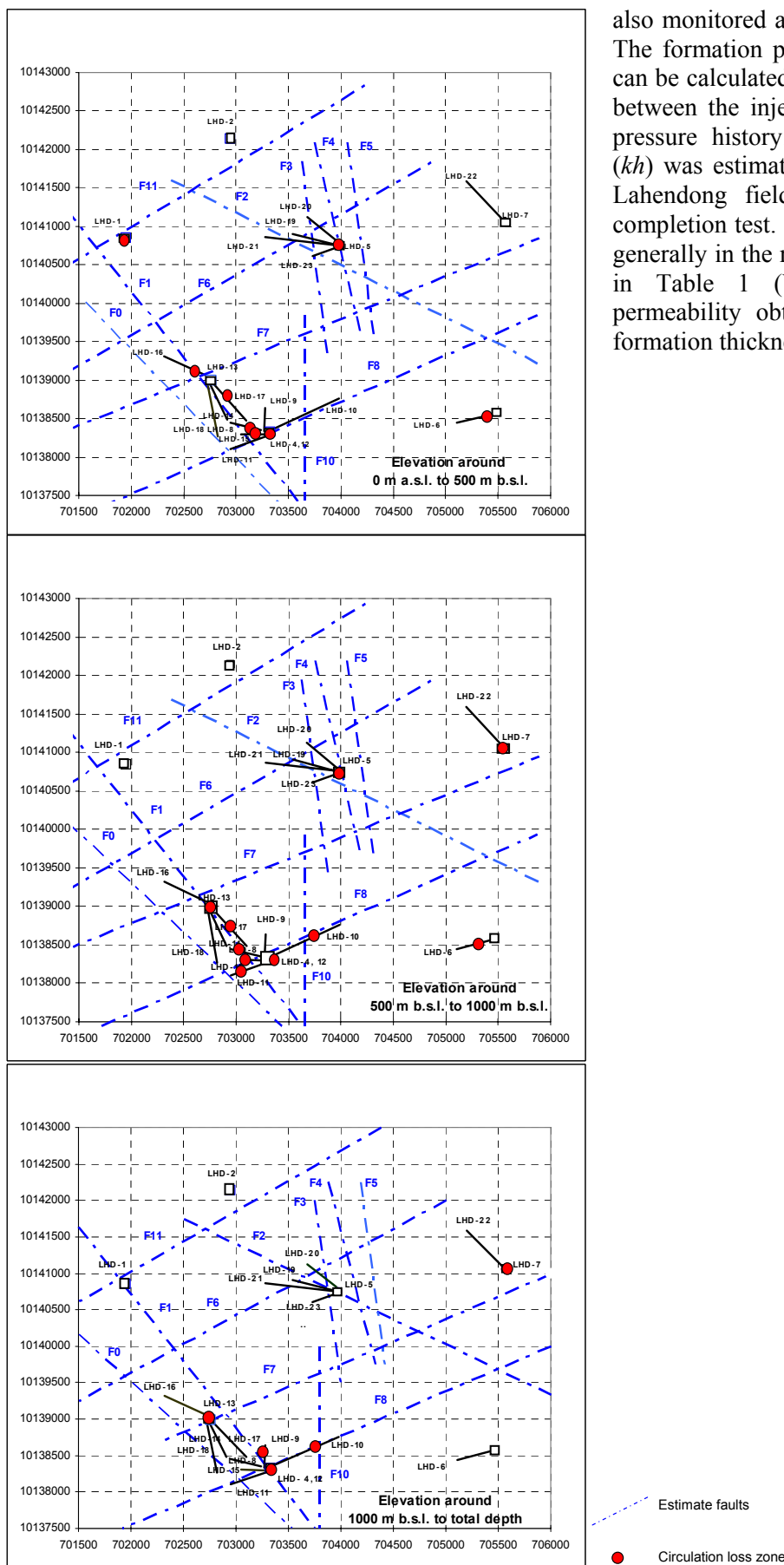


FIGURE 8 : Circulation loss zones at three depth ranges in Lahendong

also monitored after injection termination. The formation permeability near the well can be calculated by using the relationship between the injection rate and monitored pressure history. Permeability-thickness ( $kh$ ) was estimated for many wells in the Lahendong field by applying the well completion test. The permeability ( $k$ ) was generally in the range of 1-50 mD, as seen in Table 1 (Yani, 2006), with the permeability obtained by estimating the formation thickness.

TABLE 1: Permeability data available from Lahendong wells (Yani, 2006)

Well no.	$kh$ (Dm)	$h$ interval (m)			Length of $h$ (m)		$k$ (D)		Average $k$ (m <sup>2</sup> )	
		Main		Other	Main	Other	Main	Other		
LHD-1	0.2	900	1100	650	850	200	200	0.0010	0.0010	$1.0 \times 10^{-15}$
LHD-4	5	2200	2250	1650	2150	50	500	0.1000	0.0100	$5.5 \times 10^{-14}$
LHD-5	5.4	1550	1700	1100	1500	150	400	0.0360	0.0135	$2.5 \times 10^{-14}$
LHD-6	1.25	1846	1898	1051	1225	52	174	0.0240	0.0072	$1.6 \times 10^{-14}$
LHD-7	10.36	2000	2050	1500	1600	50	100	0.2072	0.1036	$1.6 \times 10^{-13}$
LHD-8	0.64	1183	1350	-	-	167	-	0.0038	0.0000	$1.9 \times 10^{-15}$
LHD-10		2300	2350	1975	2050	50				
LHD-11	4.5	1625	1700	1325	1625	75	300	0.0600	0.0150	$3.8 \times 10^{-14}$
LHD-12	5.1	1500	1800	-	-	300	-	0.0170	0.0000	$8.5 \times 10^{-15}$
LHD-13	0.56	1850	1900	1725	1850	50	125	0.0112	0.0045	$7.8 \times 10^{-15}$
LHD-15	6.44	1250	1575			325	0	0.0198	0.0000	$9.9 \times 10^{-15}$
LHD-17		1250	1550			300				

## 2.4 Discharge tests

Discharge test data from wells in the Lahendong field are given in Table 2 (PT. Pertamina, 2006) and Figure 9. The wellhead pressure of the discharging wells was about 14.7 bar-g. According to the tests, well LHD-12 gives a total mass flow of 26 kg/s with a steam ratio of 50 % (Figure 10). Wells in pad LHD-4 have a high steam ratio, or 70-90% on average and wells in pad LHD-5 have a relatively low steam ratio, or 50% on average at 14.7 bar-g wellhead pressure. The data indicates that the wells on the two pads have different discharge characteristics.

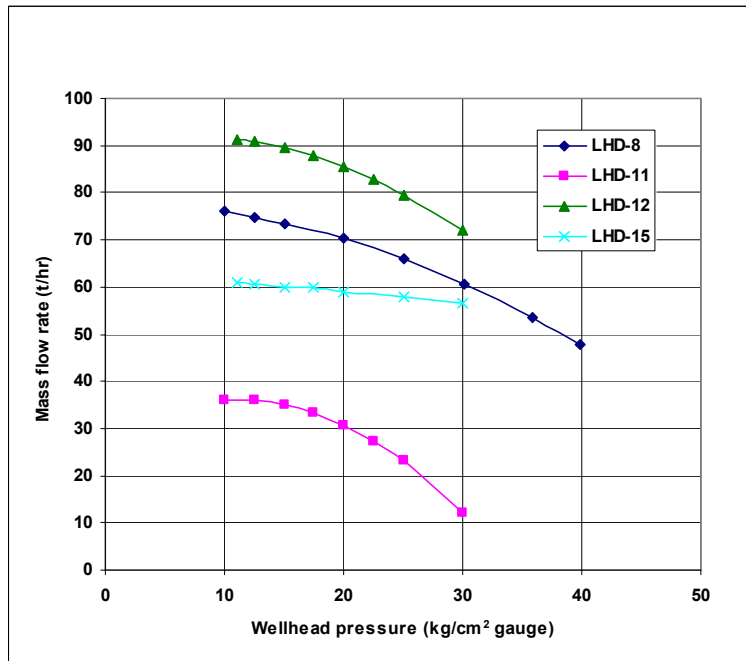


FIGURE 9: Discharge curves for wells in pad LHD-4

TABLE 2: Well discharge test data from wells in the Lahendong geothermal field

Well no.	Wellhead pressure		Steam mass flow (kg/s)	Steam ratio (%)	Total mass flow (kg/s)
	(bar-g)	(kg/cm²-g)			
LHD-8	14.7	15	18	90	20
LHD-11	14.7	15	9	80	11
LHD-12	14.7	15	13	50	26
LHD-13	14.7	15	14	90	16
LHD-10	14.7	15	6	80	8
LHD-5	14.7	15	4	30	14

After production in the field started in June 2001, there is no record of discharge tests from the wells. The only discharge data available is the total discharge from all the production wells combined through the separator unit. Wellhead pressures and temperatures are monitored continuously and recorded. Wellhead pressure during the operation of Unit I, for 20 MWe, is on average 40-50 bar-g, with a maximum wellhead opening of about 30-40%.

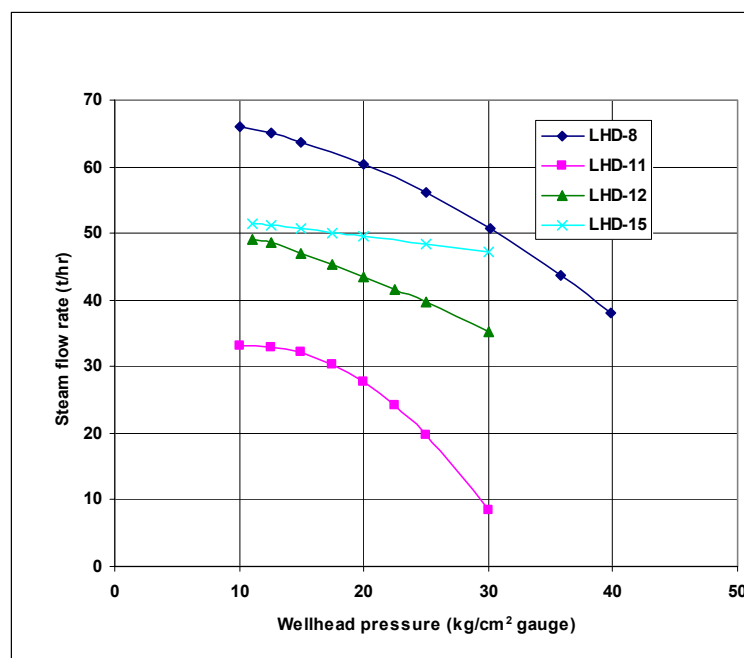


FIGURE 10: Steam flow rates in pad LHD-4

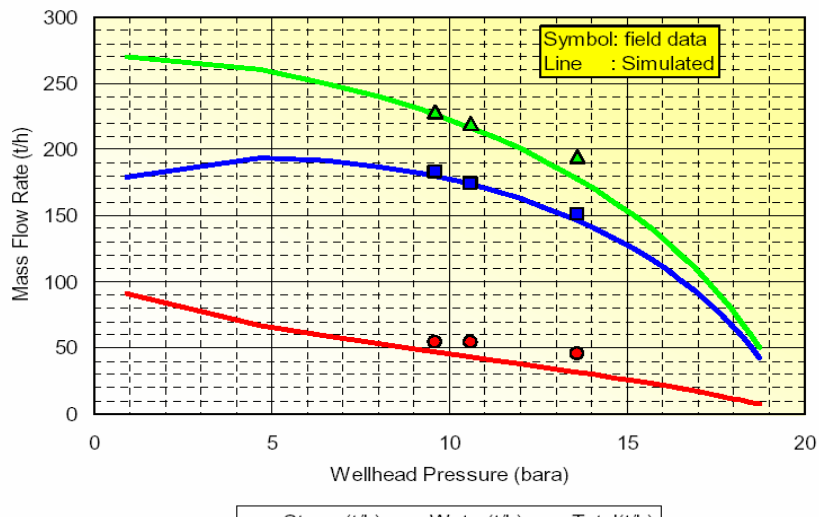


FIGURE 11: Well characteristic curves for well LHD-5

### 3. CONCEPTUAL MODEL OF THE LAHENDONG GEOTHERMAL SYSTEM

Based on the analysis of the geological structures, geochemistry, subsurface temperature and pressure conditions, a conceptual model of Lahendong geothermal field was developed. It is shown in Figures 12 and 13. The update of the pressure and temperature data from the wells in pad LHD-5 agrees with the conceptual model of this area.

A downflow (recharge) area is recognized around well LHD-7, situated on the northern slope of Mt. Tampusu. Considering this, it is deduced that the origin of geothermal fluids and spring waters should be meteoric water recharged from the mountains surrounding this field.

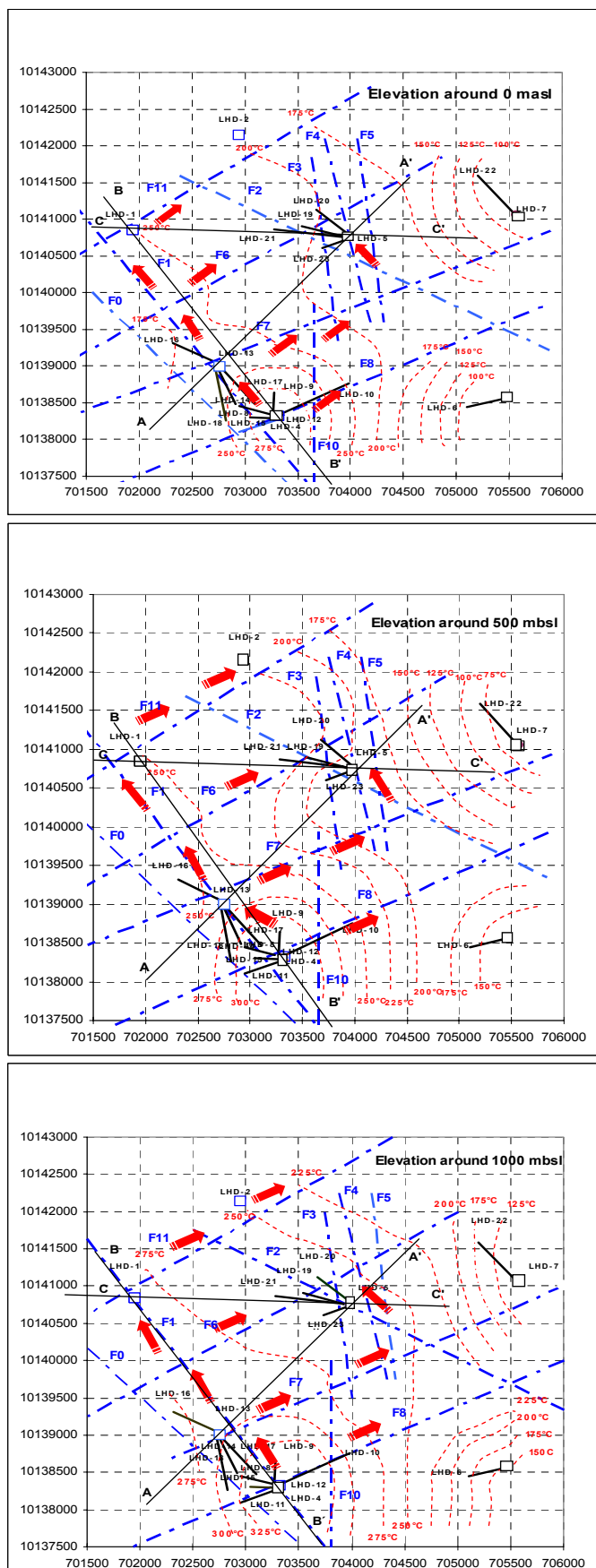


FIGURE 12: Conceptual reservoir model of the Lahendong geothermal field at three depths

The distribution of underground temperatures indicates that a main heat source or upflow area of the geothermal system is near drill pad LHD-4. The parental fluid flows up around the intersection of fault F1 with fault F8 near drill pad LHD-4, and extends to the northwest (around drill pad LHD-13) along fault F1, and northeast along fault F7. The temperature of this part of the reservoir is 330-350°C. Considering measured pressures in the wells drilled from pad LHD-4, the fluid is in single-phase condition (liquid phase), but its temperature-pressure condition is close to a two-phase condition. The same fluid flow is found through the intersections of faults F1-F7, F1-F6 and F1-F11.

Cool water flows from southeast to northwest (towards drill pad LHD-5) and mixes with the hot water flow from the southwest to northeast. The reservoir water is cooled and diluted by the cold water in the flowing process. The cold and diluted water flows down into the deep reservoir around drill pad LHD-5. The reservoir around pad LHD-5 has temperatures higher than 253°C.

The re-injection well LHD-7 was drilled near fault F7, though it is not considered to cross the fault. It is thought that a certain amount of re-injected water flows south from this field, along fault F7.

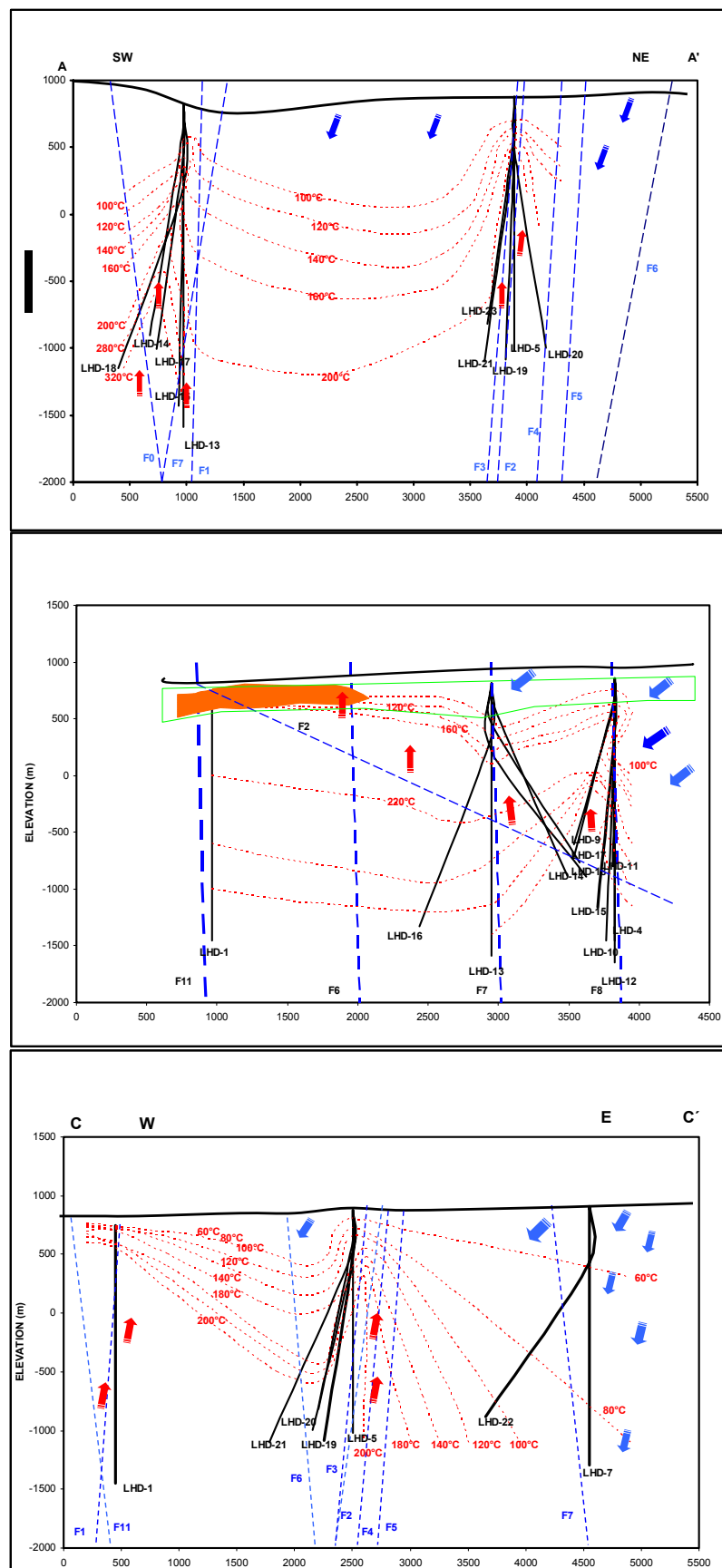


FIGURE 13: Reservoir cross-sections showing the conceptual model of the geothermal reservoir; locations of cross-sections can be found on Figure 12

#### 4. METHODOLOGY OF THE RESERVOIR SIMULATION STUDY

Computer modelling of geothermal systems has become a mature technology with application to more than 100 fields worldwide. In this chapter the author will present the Lahendong simulation study, which consists of describing the numerical modelling methodology, construction of the Lahendong numerical model (grid design, boundary and initial condition), natural state model calibration and future forecast for a given production scenario.

##### 4.1 Methodology of numerical modelling

In reservoir simulations, numerical methods are used to simulate the performance of the reservoir either at natural state conditions or under a variety of exploitation schemes. In the method used here, the observed reservoir conditions are simulated by a 3-D numerical model which consists of a number of interconnected cells or blocks. The models use the model parameters of the reservoir rocks, such as permeability, porosity, and head conduction to calculate the temperature, pressure, reservoir fluid properties and heat and mass flows in all the blocks. The model parameters are based on geological, geochemical, geophysical and well measurement data.

For this study the TOUGH2 program was used, which was developed at Lawrence Berkeley Laboratory, coupled with a user interface developed by Kamojang and the Institute of Technology, Bandung.

##### 4.2 TOUGH2 reservoir simulation

The acronym TOUGH means Transport Of Unsaturated Groundwater and Heat. It is a program for the simulation of multi-dimensional mass and heat flow for multi-component and multi-phase fluids in porous and fractured media. It belongs to the MULCOM family of numerical simulators developed at Lawrence Berkeley National Laboratory (LBNL), USA (Pruess et al., 1999). The first version of the program, TOUGH, was developed in 1983-1985 and made commercially available in 1987. TOUGH2 was released to the public in 1991 and updated in 1994, allowing more complex simulations and faster calculations than TOUGH. TOUGH2 is written in Fortran 77, and was developed under a UNIX based operating system.

The TOUGH2 program was primarily developed for studies of nuclear waste isolation, but now the spectrum of its applications is much wider. The TOUGH2 release in 1991 included five modules for different fluid properties, or EOS-modules (equations of state):

- EOS1: water, water with tracer;
- EOS2: water, CO<sub>2</sub>;
- EOS3: water, air;
- EOS4: water, air, with vapour pressure lowering; and
- EOS5: water, hydrogen.

The new version of TOUGH2 contains updated versions of these modules as well as a number of new fluid property modules. In this work, the EOS1-module is used.

The governing equations of the TOUGH2-simulator are mass- and energy-balance equations since heat and mass transfer are being simulated. The concept behind the modelling approach (porous fractured medium) involves simulating with a set of elements connected to each other. Mass and heat accumulated in each element, mass and heat flow through boundaries of elements, and possible mass/heat sinks/sources (inflow, wells, hot springs) are defined. Therefore, mass- and energy-balance equations for each element having volume  $V$  are written as (Pruess et al., 1999; Björnsson, 2003):

$$\frac{d}{dt} \iiint_V M^{(\kappa)} dV = \oint_{\Gamma} F^{(k)} \cdot \vec{n} d\Gamma + \iiint_V q^{(\kappa)} dV \quad (1)$$

1                    2                    3

where Term 1 accounts for mass/heat accumulation in element (volume)  $V$ ;  
 Term 2 gives mass/heat flow through the surfaces of element  $V$ ; and  
 Term 3 contains sinks/sources of heat and mass.

The index  $k$  may be equal to 1 for water, 2 for air, 3 for heat, and 4 for tracer, etc. (in the above equation as well as the ones below, the index  $k$  is written both as a capital and a small letter).

Mass and heat accumulation in volume  $V$  are given by:

$$M^{(\kappa)} = \phi \sum_{\beta=l,g} S_{\beta} \rho_{\beta} X_{\beta}^{(\kappa)} \quad k=1,2,3... \quad (2)$$

$$M^{(\kappa)} = (1-\phi) \rho_R C_R T + \phi \sum_{\beta=l,g} S_{\beta} \rho_{\beta} X_{\beta}^{(\kappa)} \quad (3)$$

where  $\phi$  = Porosity;  
 $S_{\beta}$  = Saturation of phase  $\beta$ ;  
 $\rho_{\beta}$  = Density ( $\text{kg/m}^3$ ); and  
 $X_{\beta}^{(k)}$  = Mass fraction of component  $k$  present in phase  $\beta$ .

The mass and heat flow are given by:

$$F^{(\kappa)} = \sum_{\beta=l,g} F_{\beta}^{(\kappa)} \quad (4)$$

$$F^{(\kappa)} = -K \nabla T + \sum_{\substack{\beta=l,g \\ k=1,2}} h_{\beta}^{(\kappa)} F_{\beta}^{(\kappa)} \quad (5)$$

where

$$F_{\beta}^{(\kappa)} = -k \frac{k_{r\beta}}{\mu_{\beta}} \rho_{\beta} X_{\beta}^{(\kappa)} (\nabla P_{\beta} - \rho_{\beta} g) \quad (6)$$

Note that all equations are non-linear, therefore, they can only be solved using numerical methods.

In simulating a geothermal reservoir, it is usually assumed that there is one component fluid only (water). In that case, there are 2 equations of 2 unknowns for each element. Unknowns are pressure and temperature (in single-phase conditions); or pressure and saturation (in 2-phase conditions). Therefore, for a system of  $N$  elements, there is a  $2N$  equation system of  $2N$  unknowns. This equation system is solved by a Newton-Raphson iteration scheme (Pruess et al., 1999; Björnsson, 2003).

### 4.3 Numerical model design

The main steps required for numerical modelling are constructing the numerical model according to the conceptual model of the reservoir, numerical grid design, specifying the rock parameters (rock properties) of the grid elements, as well as boundary conditions and source-sink distribution. Large complex three-dimensional models having computational meshes with more than 4000 block are now used routinely worldwide (O'Sullivan et al., 2001).

The parameters quantified for each grid block are volume, area of contact and nodal distance between each grid block and all adjoining ones, elevation, porosity, permeability in 3 mutually perpendicular directions (generally 2 horizontal and 1 vertical), density of the rock matrix, thermal conductivity of the rock matrix, specific heat of the rock matrix, water/steam relative permeability characteristics, water/steam capillary pressure characteristics (capillary pressure is assumed to be zero), temperature, pressure, and steam saturation (or enthalpy).

Two important factors in modelling a geothermal system are the model size and the boundary conditions to be applied on the sides of the model. Constant pressure and boundary conditions instead of flow boundary conditions have been used for modelling a hot water or liquid-dominated, two phase system. This procedure works satisfactorily but should be used with care as it may lead to spurious quasi steady-state in future scenarios where the unlimited recharge from a constant pressure boundary matches the specified production rate (O'Sullivan et al., 2001).

#### 4.4 Calibration natural state, history matching and forecast

A general procedure for model calibration has been developed. It consists of natural state modelling followed, if possible, by history matching. There are two steps. The temperature distribution and surface outflow of heat and fluid (water and steam) in the model are compared with measured field data and the permeability structure of the model is adjusted to achieve a satisfactory match. The calibration of natural state may require many iterations before a good match to the field data is achieved.

For hot water systems where the injection zone is well separated from the production zone, the production enthalpies change slowly. Therefore, for reservoirs with only a few years of production history, enthalpies may not be useful for calibration. Similarly, in vapour-dominated systems, production enthalpies remain almost constant and pressure changes slowly, so calibration by history matching is not possible if only a short production history is available (O'Sullivan et al., 2001).

The process of model calibration both for natural state matching and past history matching is difficult and time consuming. It is sometimes difficult to decide which part of a model structure should be adjusted to improve the match to a particular field measurement.

### 5. NUMERICAL MODELLING OF THE LAHENDONG FIELD

#### 5.1 Grid structure, boundary and initial conditions

The geometric configuration used in numerical simulation of the Lahendong geothermal system is shown in Figures 14 and 15. The model covers an area of  $121 \text{ km}^2$  (11 km in a NE-SW direction and 11 km in a NW-SE direction) which is larger than the known geothermal area. This large area is required to ensure a reasonable representation of the overall geological framework of the geothermal system and to reduce the effects of the boundary conditions in the model simulation. The grid design consists of sixteen different layers which are devised to represent the reservoir in the "z" (depth) direction. Each of the 16 layers is divided into 23 rows (NE-SW, x direction) and 20 columns (NW-SE, y direction). Thus, there are 460 elements per layer for a grand total of 7360 active elements in the 16 layers and 20,196 connections. The numbering of elements is per consecutive column from southwest to northeast and sequentially following the subsequent rows from southeast to northwest in each layer. The naming of layers is from top (AA) to bottom (PP).

Boundary conditions are an important part of the numerical model since they define the recharge and discharge areas which govern the natural state conditions along with sinks and sources. Constant

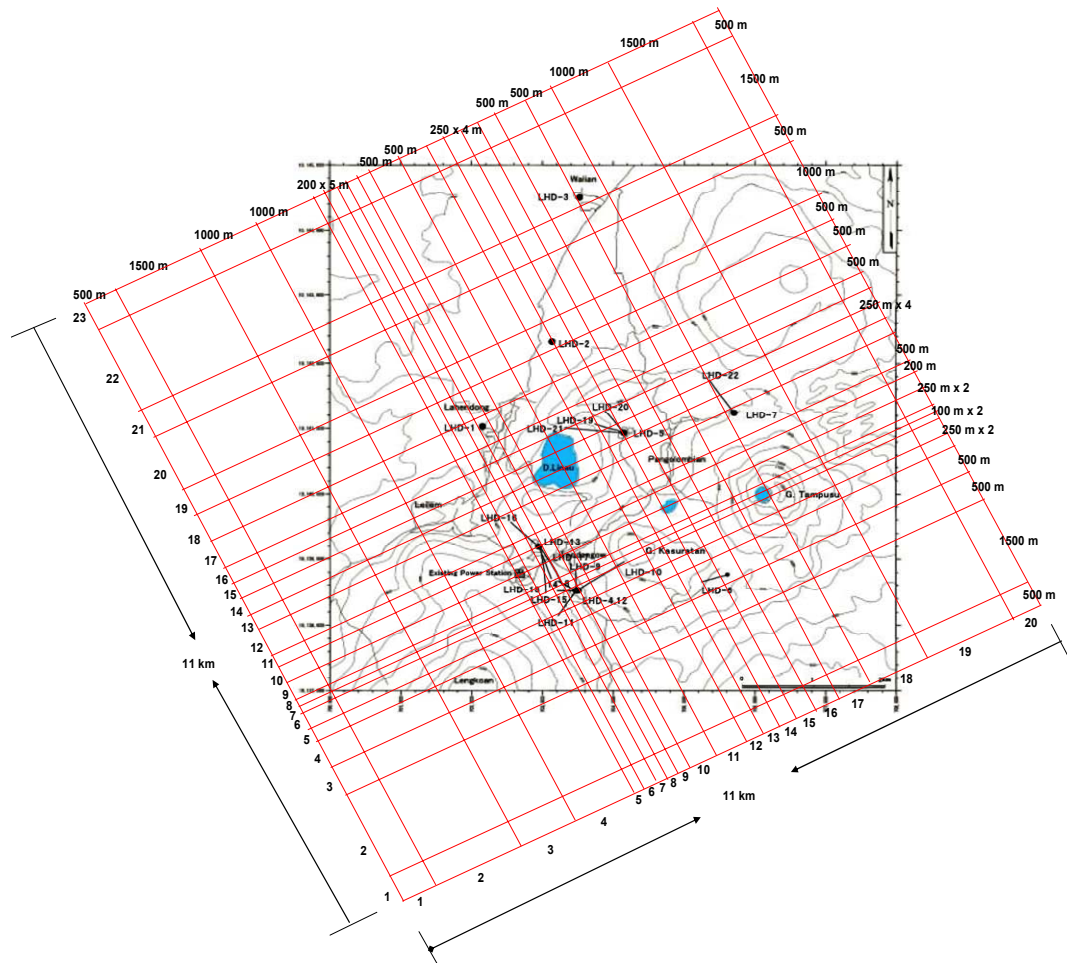


FIGURE 14: Plan view of the Lahendong numerical grid design

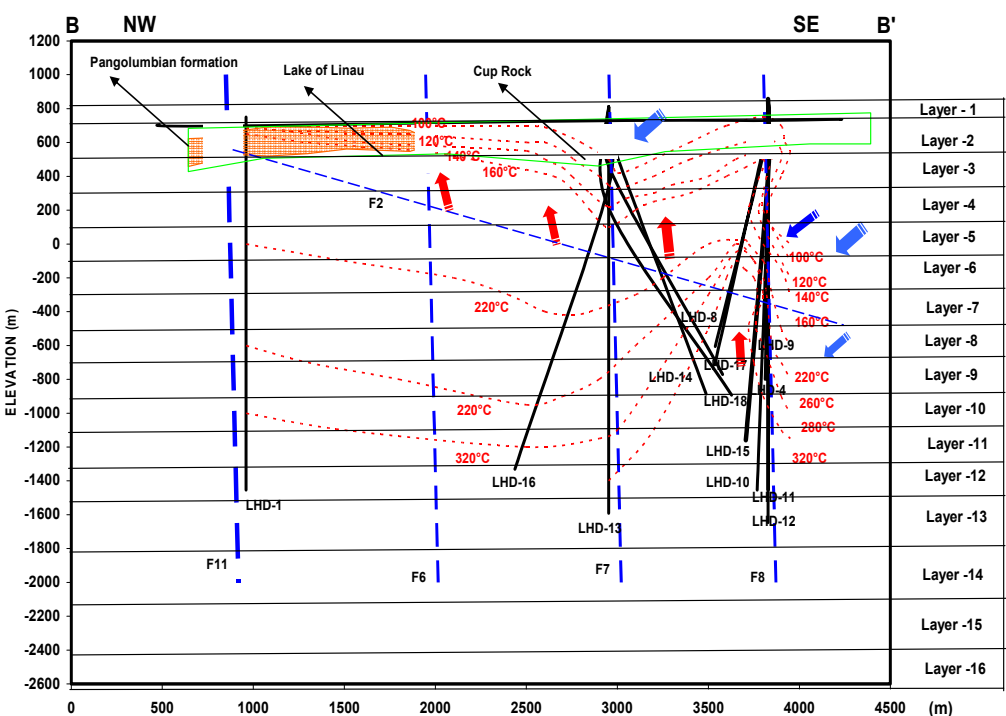


FIGURE 15: Cross-sectional view of the Lahendong numerical grid design

pressure boundary conditions were applied in this model. The top and bottom boundaries have constant pressure and temperature boundaries. There is however, no flow through these layers into the model since the vertical permeability is set close to zero. The side boundaries were also given constant pressure and temperature to give lateral recharge to the main reservoir area. The temperature is held constant by assigning high heat capacity to the sides.

An initial temperature condition is given by a constant temperature gradient  $9^{\circ}\text{C}/100\text{ m}$  from the top to the bottom layer. The temperature gradient is taken from the rock temperature gradient outside the reservoir area. The initial pressure distribution is hydrostatic, and depends on the temperature. It was calculated by the program PREDYP by assuming water level at the surface (Arason et al., 2003).

## 5.2 Natural state results for the Lahendong field

Natural state simulations were done by running the model with all blocks initially at gradient temperature and with the specified boundary conditions and heat and mass withdrawals driving the model. The simulations continue until the reservoir is stable and there are no appreciable changes with time. In this case, natural state models were run for 530 time steps which correspond to approximately 40,000 years. The steady-state conditions attained are then compared to the pre-exploitation state of the reservoir, as indicated by pressure and temperature profiles observed in wells. After many iterations and systematically adjusting a few parameters, a satisfactory match between model results and field data was obtained. In this chapter the natural state of Lahendong geothermal field is presented, and input data properties, source-sink and calibration of the natural state are discussed.

### 5.2.1 Input data for rock properties

All relevant parameters for each grid block were estimated from observed or inferred data. The available data is considered for the representative values of rock properties and they are used as inputs for the model. If no observed or inferred data was available, a value for the parameter was assumed based on knowledge of similar geothermal systems in Indonesia. The porosity value was assumed to range between 5-22%, based on the field data and typical rock properties. The value for specific heat used in the model was  $1000\text{ kJ/kg}^{\circ}\text{C}$ . The thermal conductivity of the water-saturated rocks in the reservoir ranges from  $1.98$  to  $3.46\text{ W/m}^{\circ}\text{C}$ . The relative permeability was specified in the model using Corey type curves (Pruess et al., 1999). The initial permeability distribution was based on available results from well test analyses. These values were modified during the natural state modelling to obtain sub-surface temperature matches.

The main objective of the natural state calibration is to verify the temperature and pressure distributions and the heat/mass flow aspects in the model. In this context, the major rock properties of importance are permeability and thermal conductivity. The table below (Table 3) presents the best estimates of the rock properties in the model. Examples of rock type distribution in the model grid are presented in Appendix I. Source and sink locations in the model are also described in Appendix I.

### 5.2.2 Sources and sinks

In the numerical model, sources and discharge sinks are given to maintain the thermodynamic conditions; they control the main inflows and outflows in the model. After many iterations, a good result of the natural state condition was obtained with the values of sources and discharge sinks shown in Tables 4 and 5.

Two types of sources (HU and BQ) are given in layer-15 near pad LHD-4 and LHD-1, with constant 30 and 60 kg/s flowrates and enthalpy 1500 and 1750 kJ/kg, respectively. The sources given drive the convection of heat and mass in the model from the deep heat input (layer-15) with a temperature of

TABLE 3: Rock properties of the natural state model

Layer	Name of rock type properties	Description	Porosity	Density (kg/m <sup>3</sup> )	Permeability (m <sup>2</sup> )			Heat conductivity (W/m-C)	Specific heat (J/kg-C)
					Kx	Ky	Kz		
1	Top boundary	Boundary condition at the top	0.1	2500	1.0E-18	1.0E-18	1.0E-18	2	1.00E+21
16	Bottom boundary	Boundary condition at the bottom	0.1	2500	1.0E-15	1.0E-15	1.0E-30	2	1.00E+21
1 - 16	Side boundary	Boundary condition at the all of around model	0.1	2500	1.0E-15	1.0E-15	1.0E-18	2	1.00E+21
2	Cap rock	Cap rock	0.05	2500	1.0E-18	1.0E-18	1.0E-18	2	1.00E+03
1, 2	Pangolombian formation	Rock formation	0.15	2500	1.0E-15	1.0E-15	1.0E-16	2	1.00E+03
3 - 6	Tondano formation	Rock formation	0.22	2500	5.0E-16	1.0E-15	5.0E-17	2.9	1.00E+03
5 - 15	Pre-Tondano formation	Rock formation	0.1	2500	1.0E-16	5.0E-16	1.0E-16	3.5	1.00E+03
2 - 6	Down flow area	Rock formation for defenition down flow zone	0.1	2500	1.0E-15	1.0E-15	7.0E-15	2	1.00E+03
1 - 15	PF1	Faults properties with the name PF1	0.1	2500	7.0E-15	2.0E-15	2.0E-15	2	1.00E+03
1 - 15	PF2	Faults properties with the name PF2	0.1	2500	7.0E-14	7.0E-14	5.0E-14	2	1.00E+03
1 - 12	PF3	Faults properties with the name PF3	0.1	2500	2.0E-15	5.0E-14	5.0E-15	2	1.00E+03
1 - 15	PF4	Faults properties with the name PF4	0.1	2500	5.0E-14	5.0E-15	5.0E-15	2	1.00E+03
1 - 15	PF5	Faults properties with the name PF5	0.1	2500	5.0E-14	7.0E-15	5.0E-15	2	1.00E+03
7 - 8	PF6	Faults properties associated with pad LHD-5	0.1	2500	2.0E-15	5.0E-14	1.0E-14	2	1.00E+03
14 - 15	PF7	F properties associated with pad LHD-5 at deep part reservoir	0.1	2500	1.0E-16	1.0E-16	1.0E-16	2	1.00E+03
7 - 10	PF8	Faults properties associated with pad LHD-4	0.1	2500	8.0E-15	8.0E-15	8.0E-15	2	1.00E+03
9 - 14	PF9	Upflow close to pad LHD-4	0.1	2500	1.0E-14	7.0E-15	5.0E-15	2	1.00E+03
7 - 14	PF10	Upflow close to pad LHD-1	0.1	2500	5.0E-14	5.0E-14	3.0E-14	2	1.00E+03

TABLE 4: Source definition in natural state

Cell name	Layer	Enthalpy (kJ/kg)	Rate (kg/s)
PW	2	300	10
NY	2	400	50
RF	2	250	60
HU	15	1550	30
BQ	15	1820	60
<b>Total in</b>		<b>210</b>	

TABLE 5: Sink definition in natural state

Cell name	Layer	PI (m <sup>3</sup> )	P <sub>bottom</sub> - P <sub>model</sub> (Pa)	Rate (kg/s)
OY	2	1.0×10 <sup>-8</sup>	1.0×10 <sup>-6</sup>	3.26
JD	2	1.0×10 <sup>-7</sup>	1.0×10 <sup>-6</sup>	1.48
GR	3	1.0×10 <sup>-8</sup>	2.0×10 <sup>-6</sup>	67.17
FJ	3	1.0×10 <sup>-9</sup>	2.0×10 <sup>-6</sup>	6.36
EG	3	1.0×10 <sup>-8</sup>	2.0×10 <sup>-6</sup>	131.73
<b>Total out</b>				<b>210</b>

about 380°C. The model also has three sources (PW, NY and RF) in layer-2, which simulates inflow from the surface of cool water at rates of 50, 60 and 10 kg/s with an enthalpy of 400, 250 and 300 kJ/s, respectively. They represent the downflow in the conceptual model with a temperature of about 40°C.

Three sinks (GR, FJ and EG) represent the hot spring surface manifestations around Lake Linau. The total outflow to the surface through the sinks in layer-3 totals 180 kg/s. One sink to the northeast in (OY) layer-2 represents the hot spring at that location, with an outflow of 3.26 kg/s. The last sink (JD-2) represents the hot spring at northeast LHD-2 with an outflow to the surface of 1.48 kg/s. The water that infiltrated through layer-2 is allowed to be heated up by the steam from the deep hot water. In total, 210 kg/s of water flow into and out of the model, showing that the numerical model takes a mass balance of inflow and outflow in the natural state condition.

### 5.2.3 Natural state calibration

Results of the natural state simulations are found in Appendix II. The maximum differences between the model and well data are around 20 bar for pressure and 40°C for temperature. The temperature and pressure distributions calculated for 16 different layers of the model are presented in Appendix III.

### 5.3 Forecast calculation on future production

The 20 MWe Unit I in the power plant in Lahendong started in June 2001. Because of the lack of drawdown reservoir data, history matching of past exploitation time from June 2001 to the present is

not possible. Here, the past exploitation time is considered to be a part of the future forecast. The mass production history of each production well and the re-injection history were not monitored after the commission of Unit I. However, the wellhead pressure of the production wells was monitored and the total mass flow from all of the wells combined was also monitored. Well characteristic curves were used for calculating the mass flow contributions from each well for the total steam supply to the power plant (see Section 2.4 discharge test data). The monitored changes in the wellhead pressures do not reflect the changes in reservoir pressure directly. The wellhead pressure can, therefore, not be used to simulate the reservoir drawdown due to the 20 MWe production in the field.

Due to the lack of pressure monitoring data, the production history from 2001 for Unit I is assumed a part of the future forecast. The steam for Unit I is supplied by wells LHD-8, 11, 12 and 15. The 20 MWe Unit II is scheduled for commission in the beginning of 2007 and will be supplied by wells LHD-8, 11, 17 and 18 with each well giving about 5 MWe. Unit III is expected to begin operation in the beginning of 2008 with steam supply from wells LHD-5, 19, 20, 21 and 23. The characteristics of the wells are considered to be the same as in well LHD-5. The future forecast is calculated for 30 years or until 2036. The expected production scenario from 2001 to 2036 is found in Figure 16.

In the calculations it is assumed that 2 kg/s of steam, at separation pressure, are needed to produce 1 MWe. Figure 17 shows the estimated total production from the Lahendong field from 2001 to 2036. About 241 kg/s is the estimated total mass production from the field needed to supply the 60 MWe power plant until 2036. Mass flow from each well is based on the well curve characteristics. The wastewater from the production is re-injected through wells LHD-7 and 22.

According to the forecast calculations, the reservoir pressure drawdown should be about 10 bar after 60 MWe power production for 30 years. Temperature changes at the end of the forecast are negligible. The pressure and temperature changes with time in wells in the field during the future production scenario are presented in Appendix IV. Due to limited monitoring data during production,

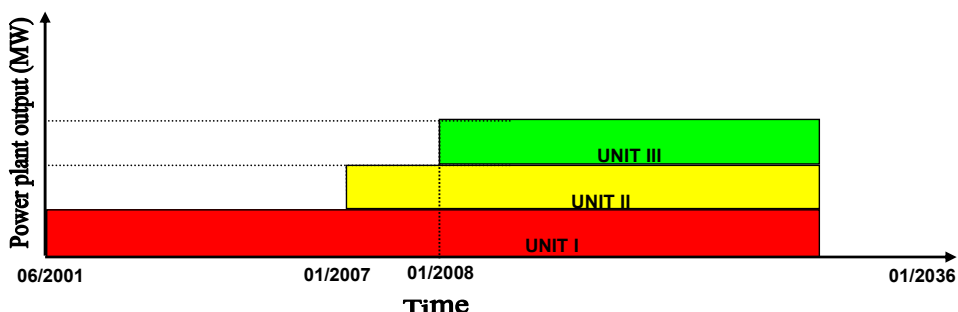


FIGURE 16: Future forecast and power output of the three Units in Lahendong

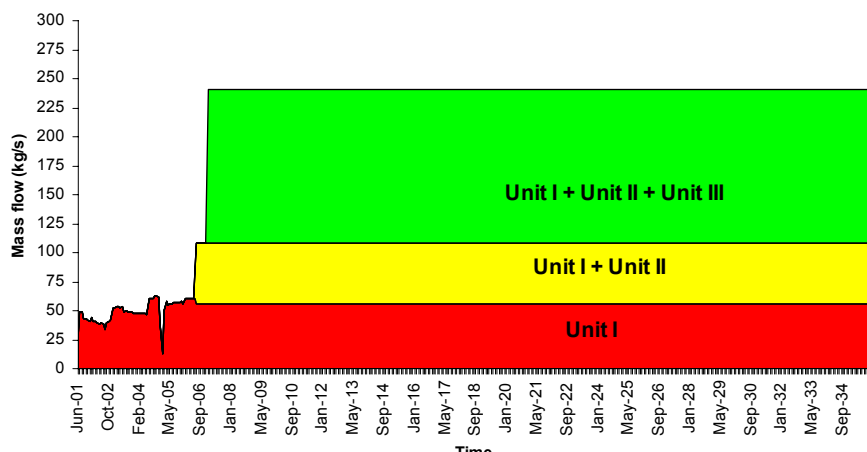


FIGURE 17: Future forecast of total mass flow for 60 MWe power production in Lahendong

no calibration on the production state of the model was performed. Therefore, the forecast is highly uncertain and should be updated as more data becomes available for model calibration. Figures on temperature and pressure distribution in the model in year 2036 are found in Appendix V.

## 6. MONITORING WATER LEVEL – PRESSURE DRAWDOWN

Management of a geothermal field entails making a decision between possible courses of action. Such decisions are based on available data on the field in question and the conceptual model. In many cases field and production data are so scarce that the uncertainties in the geothermal system's future response to production are large so any estimate is simply a guess, although some guesses will be better than others. The existence of a production monitoring history makes decision making of the field management much simpler. Many properties of the reservoir can only be subjects of conjecture in the developmental stages, but as production continues, field data accumulates and the monitoring history increases, properties of the reservoir can be estimated with numerical modelling. Detailed reservoir monitoring is, therefore, essential for successful numerical simulations in order to assess the power capacity of the resource and aid proper field management decision making.

In addition, work must be put into monitoring the performance of the wells and the surface equipment. This is necessary in order to detect irregularities that may signal the need for repair work, to measure the trends of declining performance, to anticipate the need for additional wells, to monitor a reduction in wellhead pressure and for future forecasts. Numerous problems can occur in the operation of a geothermal project, and regular monitoring is needed to ensure that they do not get out of hand.

The basic monitoring is of reservoir pressure drawdown. Pressure drawdown in a reservoir can be monitored through water level measurements and down-hole pressure measurements. Choosing wells for drawdown monitoring can include wells which stand closest to the production wells or outside the reservoir area. It could also be an unproductive well or a shallow well in the area. Regular monitoring, for example every 3 months, every 6 months or a minimum of once a year, is needed to increase the confidence in data quality.

Good numerical simulation and future forecasting results depend on data quality. The data are used to calibrate the numerical model which subsequently is used for future predictions. The future predictions are needed to answer questions about the capacity of the geothermal system and the sustainability of the project's development plan. There is a risk of over-investment in wells and surface facilities if no estimate is available on the power production capacity of the geothermal field.

## 7. CONCLUSIONS AND RECOMMENDATIONS

### 7.1 Conclusions

A three-dimensional numerical model of Lahendong geothermal system was developed. The model covers a surface area of about 120 km<sup>2</sup> and consists of over 7300 grid blocks. The natural state model was run for 530 time steps, which corresponds to approximately 40,000 years. The steady-state conditions attained were compared to the pre-exploitation state of the reservoir. The model was also used to forecast the performance of the reservoir with increased production, from 20 to 60 MWe, over a 30 year period. The main conclusions of this work are:

- A detailed TOUGH2 numerical model was developed to simulate the natural state of the field, based on the conceptual model. The model shows a fair match between calculated and observed temperature and pressure in wells in the field.
- Permeability in the main reservoir of the natural state model is in the range of 0.1-70 mD, which compares reasonably well with the results of injection tests performed in individual wells (range

of well permeability 1-55 mD). Skin effect from drilling material reduces the permeability around wells.

- A 60 MWe production scenario for 30 years was tested using the numerical model, resulting in a 10 bar pressure drawdown.
- Due to limited monitoring data during production, this forecast is uncertain and should be updated as more data becomes available.

## 7.2 Recommendations

- Reservoir monitoring is essential and should be improved in the Lahendong field.
- More data on pressure drawdown during production is needed to calibrate the model, in order to give more reliable forecasts and potential production assessments.
- The result of this work is a preliminary numerical modelling study of the Lahendong geothermal system. The model can be used for further studies if updated as more data becomes available.

## ACKNOWLEDGEMENTS

I would like to express my gratitude to the UNU staff, Dr. Ingvar B. Fridleifsson, Mr. Lúdvík S. Georgsson, Mrs. Guðrún Bjarnadóttir and Ms. Thórhildur Ísberg for their care, generous help, advice and assistance. I am much obliged to the UNU, the Government of Iceland and PERTAMINA for granting me this opportunity to improve my knowledge and skills and for giving me the opportunity to attend the UNU Geothermal Training Program in Iceland.

I am sincerely thankful to my supervisors, Mr. Arnar Hjartarson, Mr. Gudni Axelsson and Mr. Egill Júlíusson for their guidance and support during project execution. Special thanks to the entire reservoir engineering group for their dedication in imparting their expertise and knowledge.

## REFERENCES

- Arason, Th., Björnsson, G., Axelsson, G., Bjarnason, J.Ö., and Helgason, P., 2003: *The geothermal reservoir engineering software package Icebox, user's manual*. Orkustofnun, Reykjavík, report, 53 pp.
- Björnsson, G., 2003: *Numerical modelling 1 and 2 with special emphasis on the TOUGH code*. UNU-GPT, Iceland, unpublished lecture notes.
- Marihot E.P.S., Yani, A., Tesha, Kustono, H., Budi, I.M., and Nugroho, A.J., 2004a: *Drilling report LHD-17*. Pertamina Geothermal, Indonesia, internal report.
- Marihot E.P.S., Yani, A., Tesha, Kustono, H., Budi, I.M., and Nugroho, A.J., 2004b: *Drilling report LHD-18*. Pertamina Geothermal, Indonesia, internal report.
- Marihot E.P.S., Yani, A., Tesha, Kustono, H., Budi, I.M., and Nugroho, A.J., 2005a: *Drilling report LHD-19*. Pertamina Geothermal, Indonesia, internal report.
- Marihot E.P.S., Yani, A., Tesha, Kustono, H., Budi, I.M., and Nugroho, A.J., 2005b: *Drilling report LHD-20*. Pertamina Geothermal, Indonesia, internal report.
- Marihot E.P.S., Yani, A., Tesha, Kustono, H., Budi, I.M., and Nugroho, A.J., 2005c: *Drilling report LHD-21*. Pertamina Geothermal, Indonesia, internal report.

Marihot E.P.S., Yani, A., Tesha, Kustono, H., Budi, I.M., and Nugroho, A.J., 2005d: *Drilling report LHD-22*. Pertamina Geothermal, Indonesia, internal report.

Marihot E.P.S., Yani, A., Tesha, Kustono, H., Budi, I.M., and Nugroho, A.J., 2006: *Drilling report LHD-23*. Pertamina Geothermal, Indonesia, internal report.

O'Sullivan, M.J., Pruess, K., and Lippmann, M.J., 2001: *State of the art of geothermal reservoir simulation*. Geothermic, 392–429.

Pruess, K., Oldenburg, C., and Moridis, G., 1999: TOUGH2, user's guidance version 2.0. Lawrence Berkeley National Laboratory, 197 pp.

PT. Pertamina Geothermal, 2006: *Production monitoring report*. PT. Pertamina Geothermal, Indonesia, internal report.

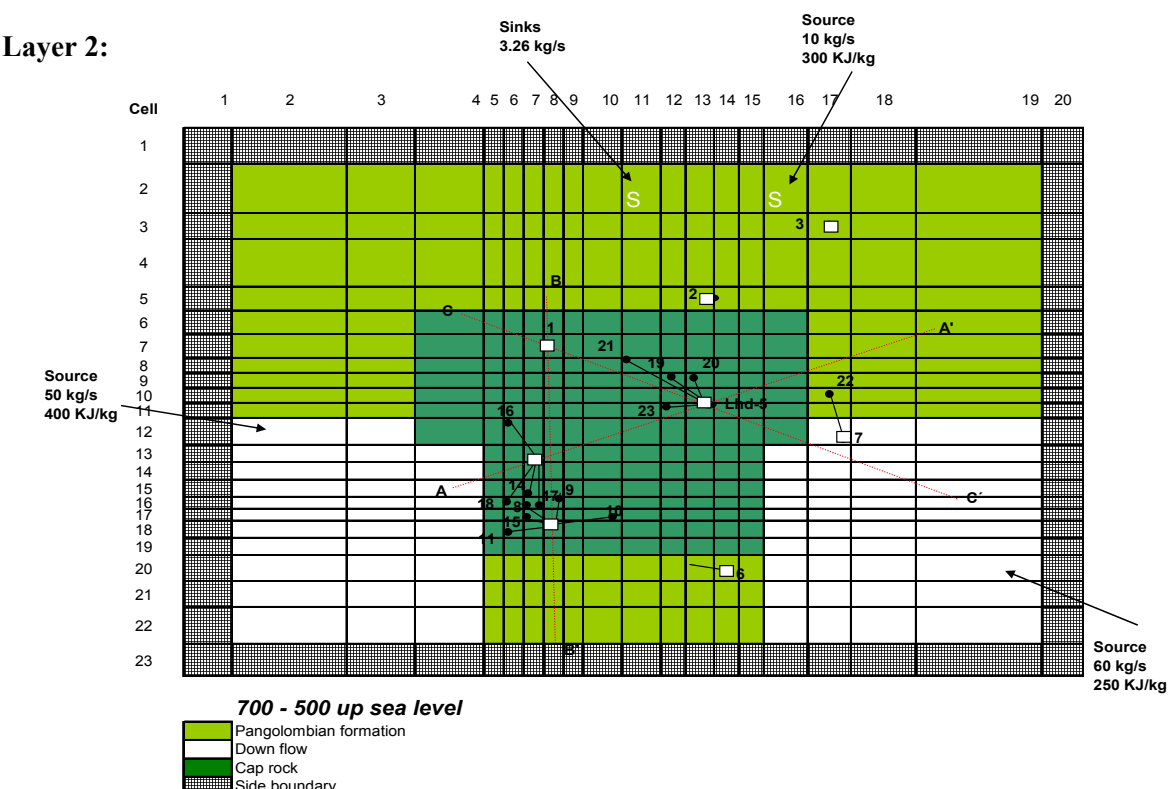
PT. PLN, 2005: *Resource study report Lahendong Geothermal*. PT. PLN, Indonesia, internal report.

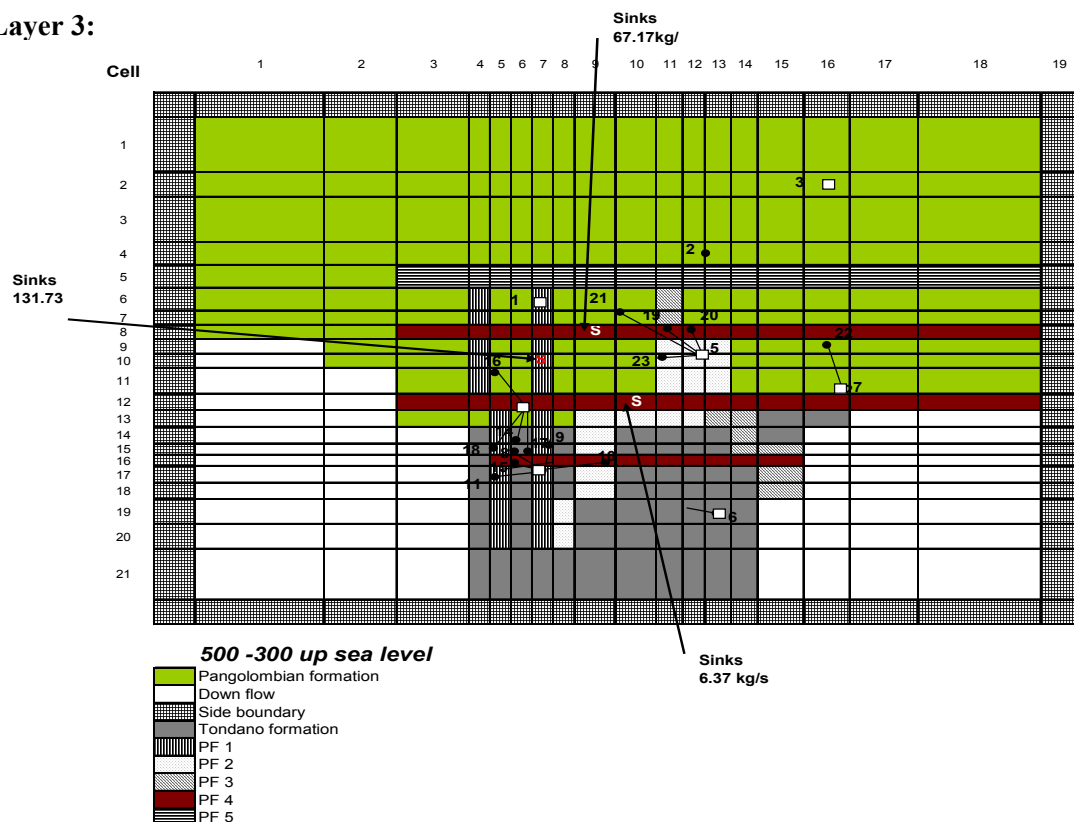
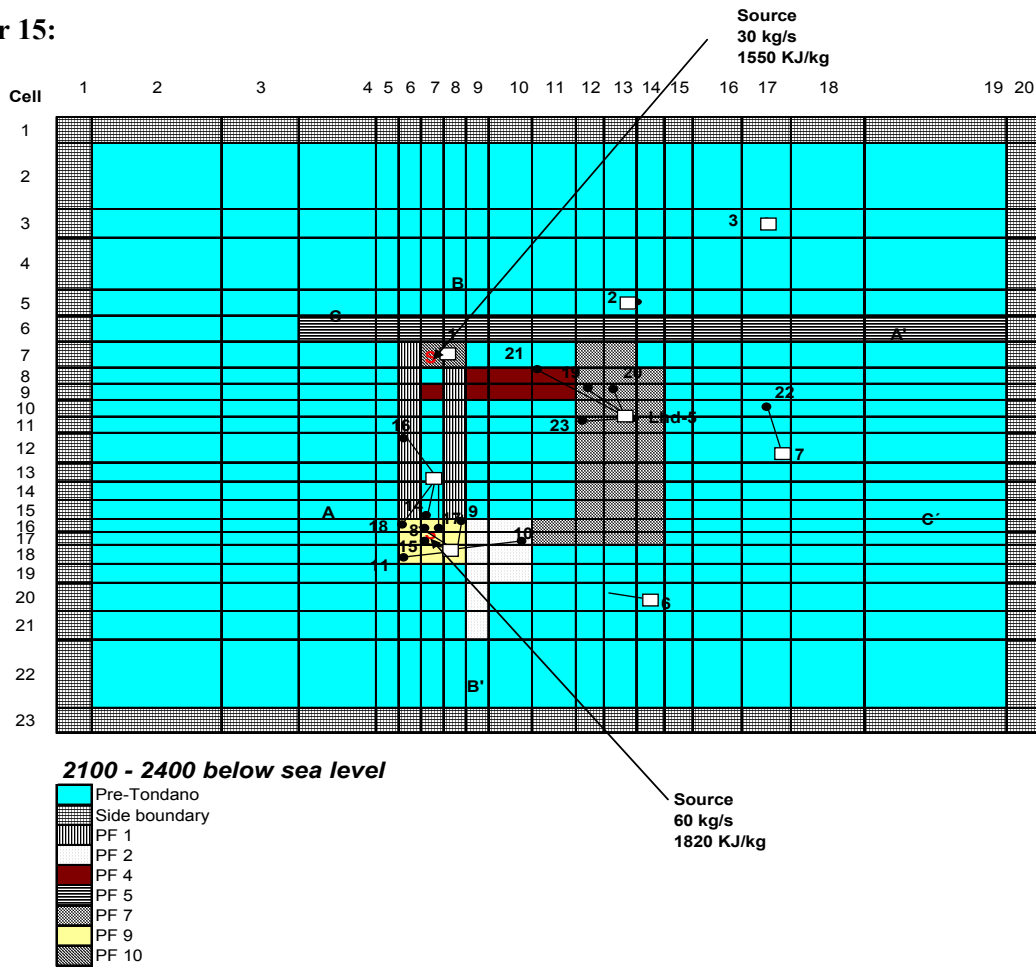
Sujata, I.K., 2006: *Update well testing data, report and analysis*. Pertamina Geothermal, Indonesia, internal report.

Siahaan, E.E., Soemarinda, S., Fauzi, A., Silitonga, T., Azimudin, T., and Raharjo, I.B., 2005: Tectonism and volcanism study in the Minahasa compartment of the north arm of Sulawesi related to Lahendong geothermal field, Indonesia. *Proceedings of the World Geothermal Congress 2005, Antalya, Turkey*, CD, 5pp.

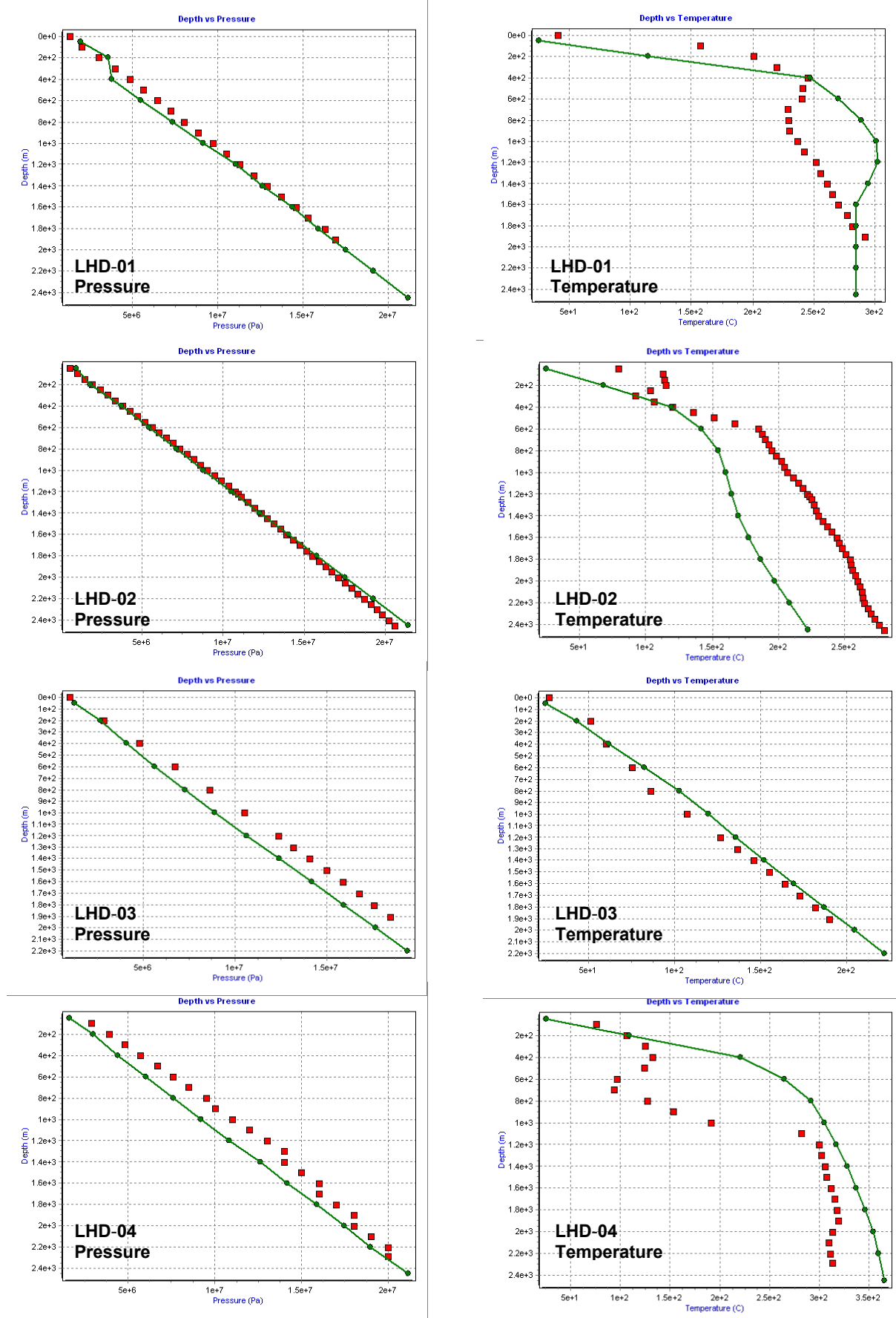
Yani, A., 2006: *Update, well and interpretation data*. Pertamina Geothermal Lahendong, Indonesia, internal report.

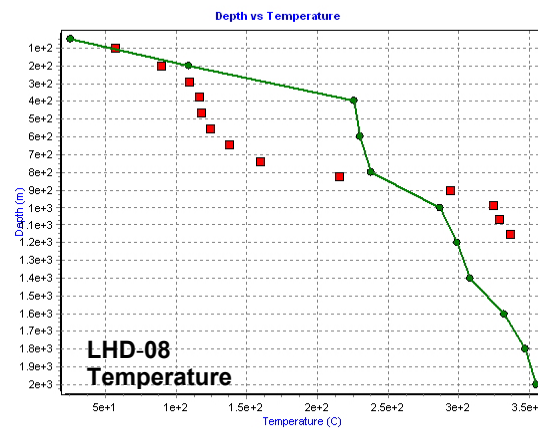
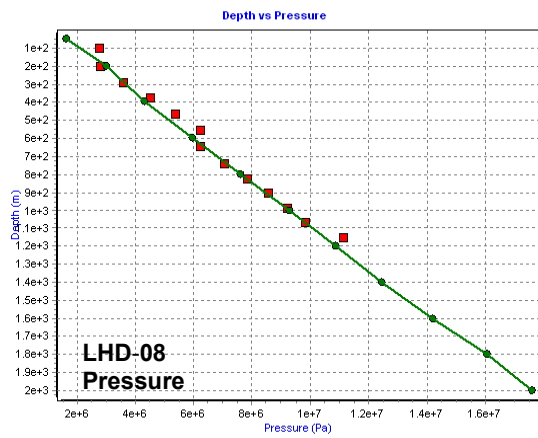
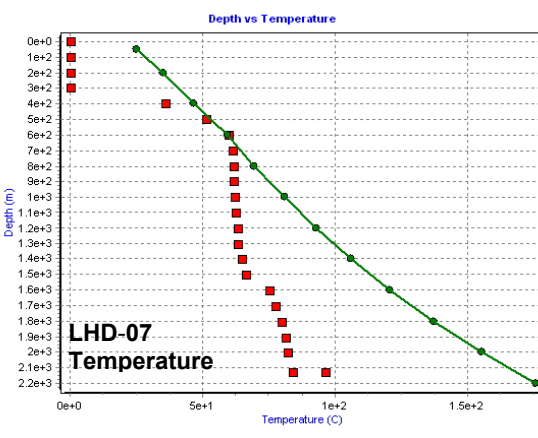
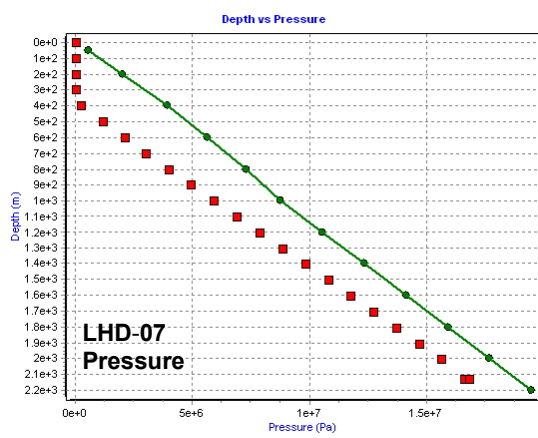
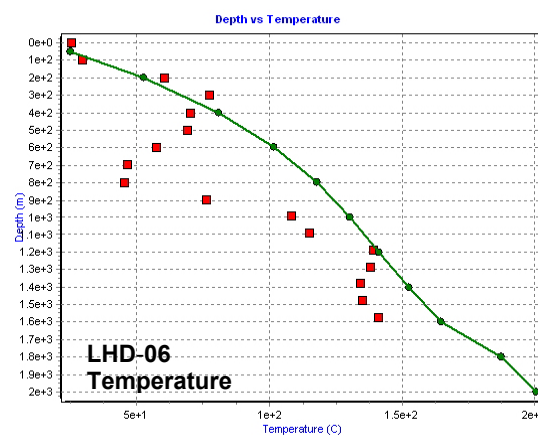
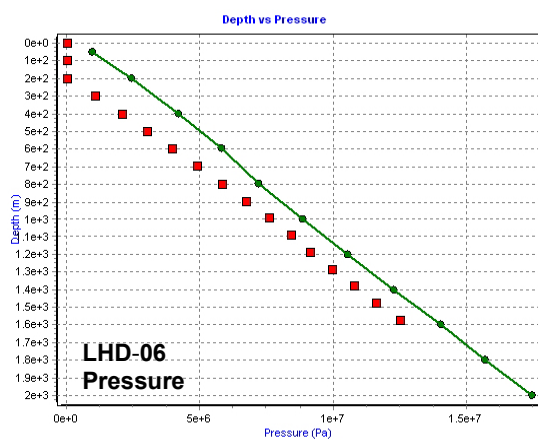
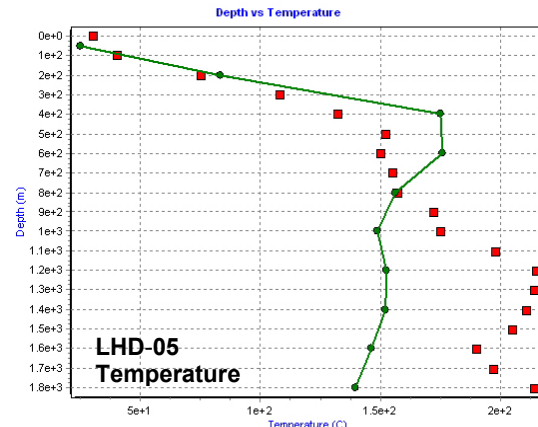
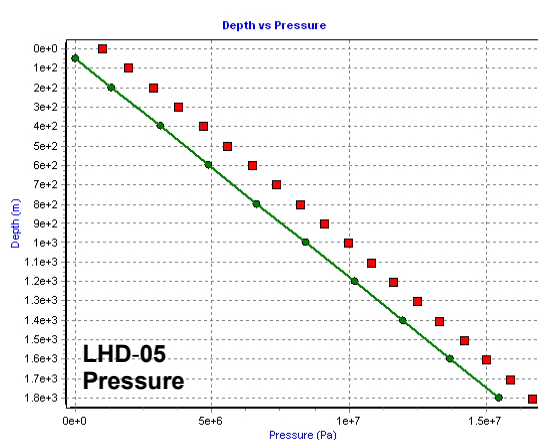
#### APPENDIX I: Source, discharge sink and rock properties in the numerical model of the Lahendong geothermal reservoir

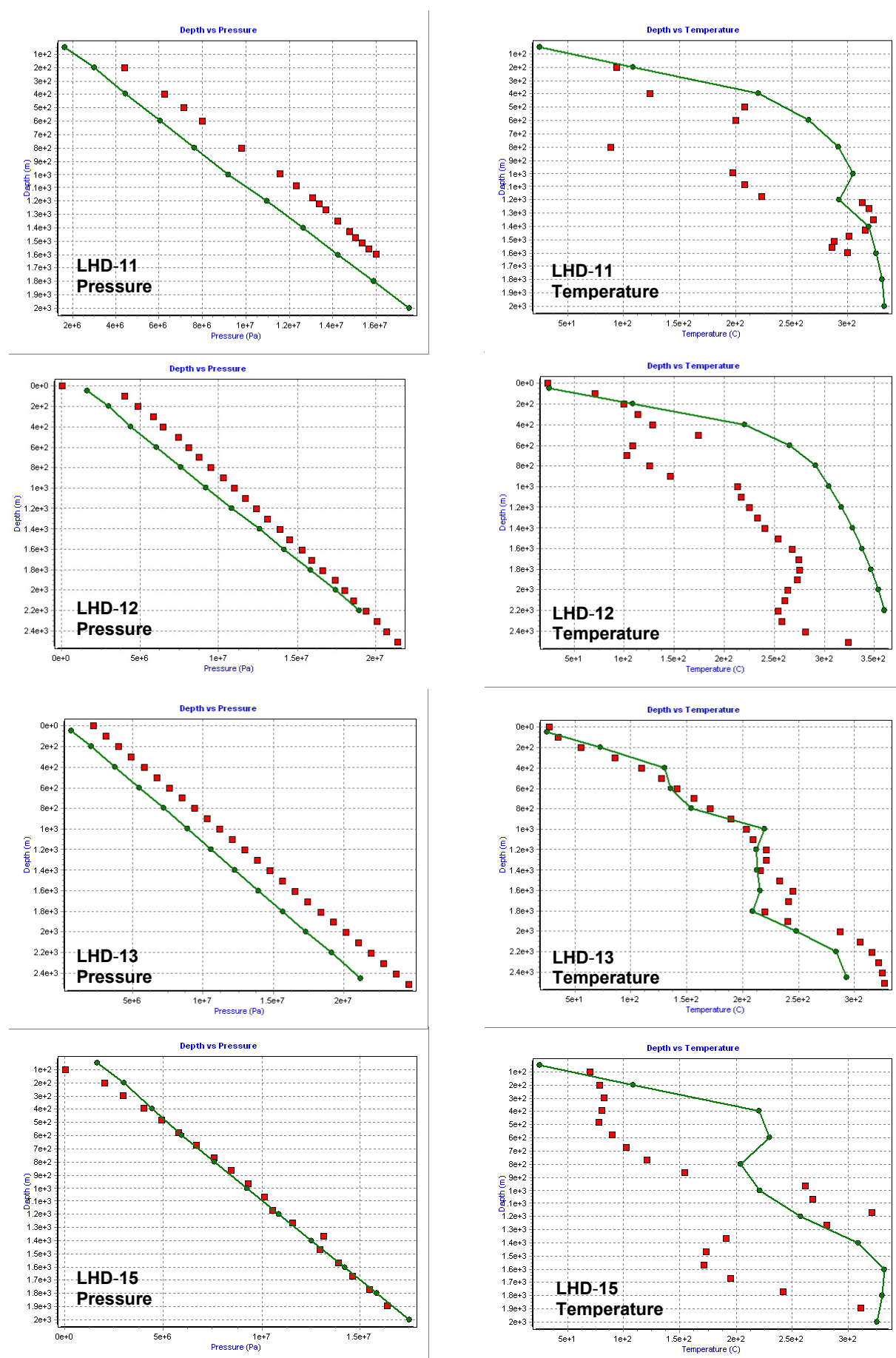


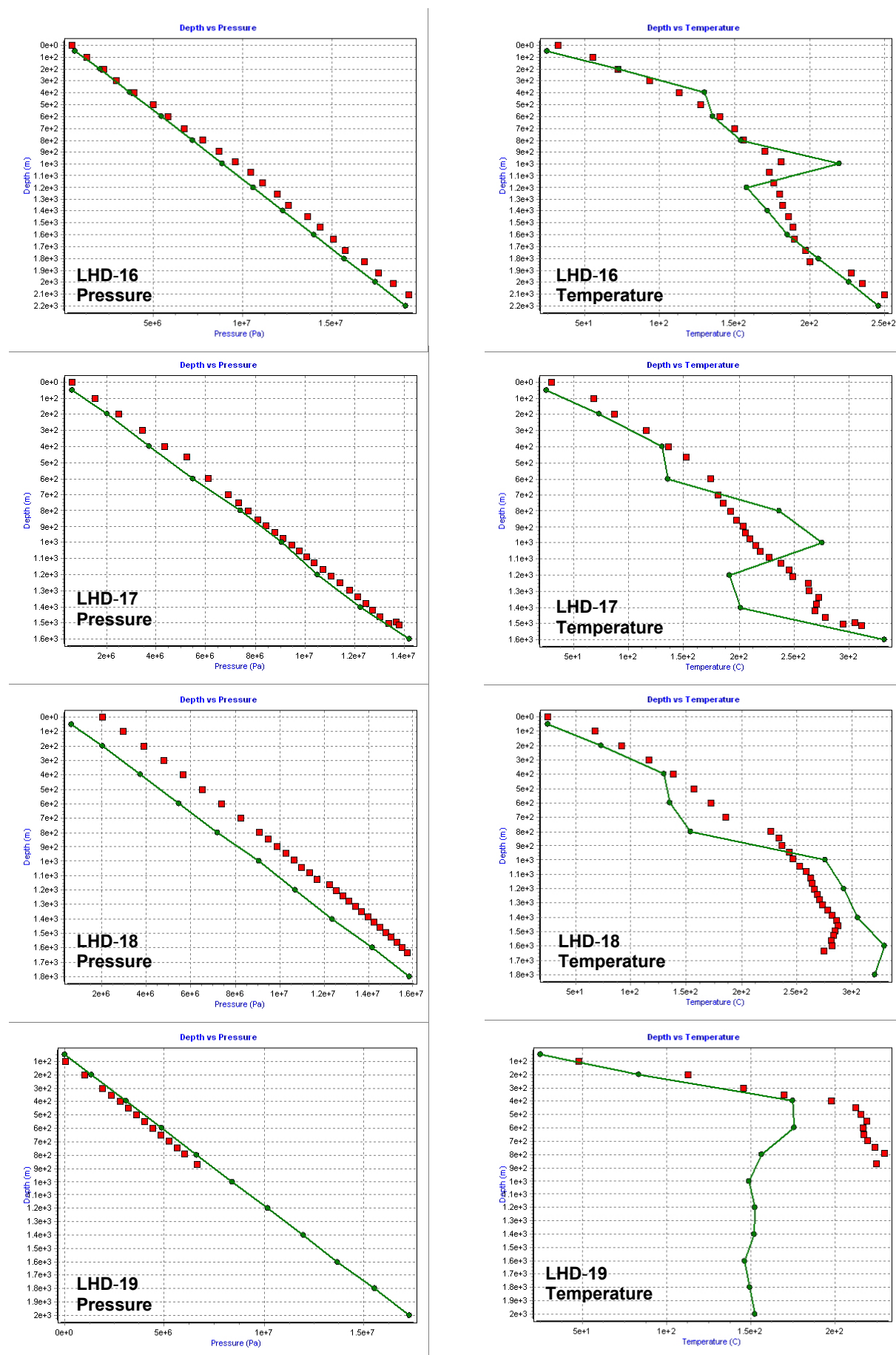
**Layer 3:****Layer 15:**

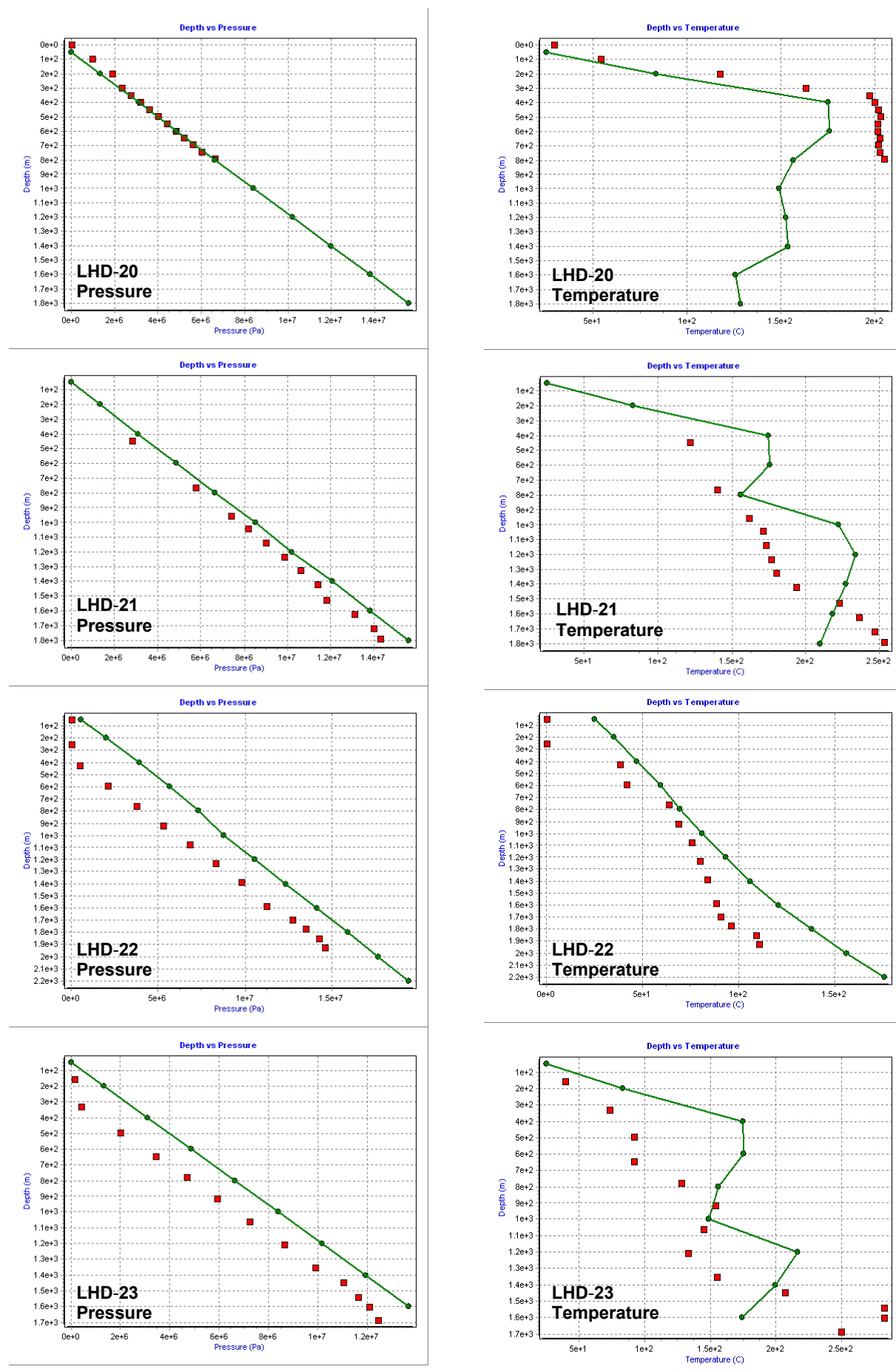
**APPENDIX 2: Comparison of measured and calculated pressure and temperature profiles in the wells in Lahendong field (rectangles (red) are data and dots with line (green) are model)**





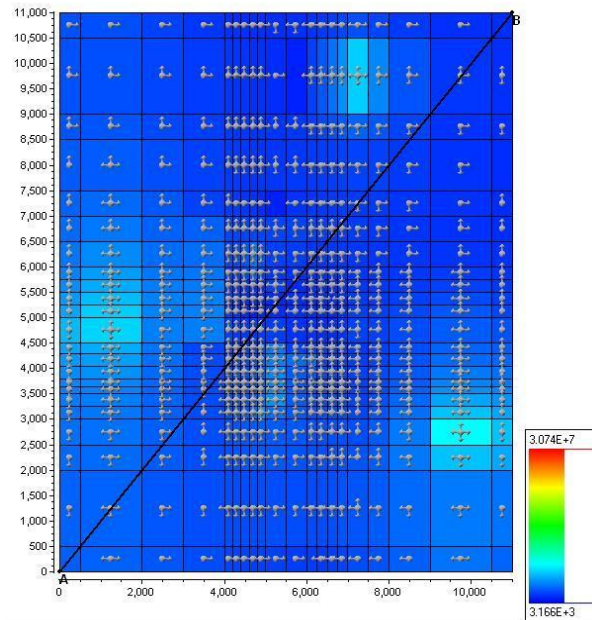




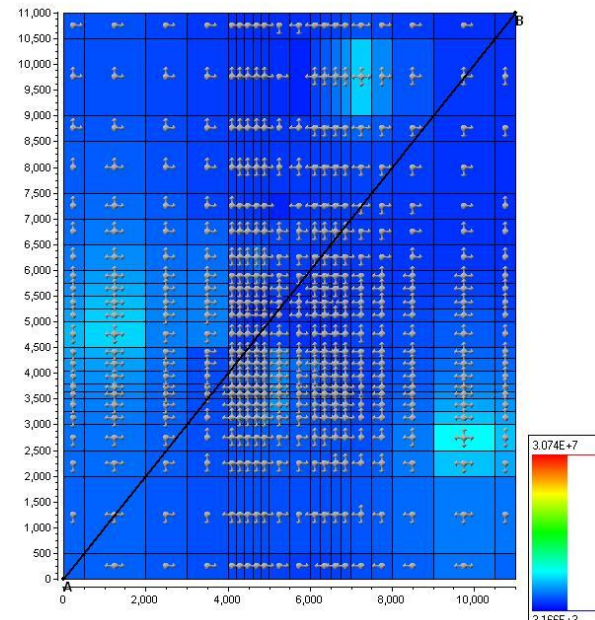


**APPENDIX III: Distribution of pressure and temperature in the natural state simulation**

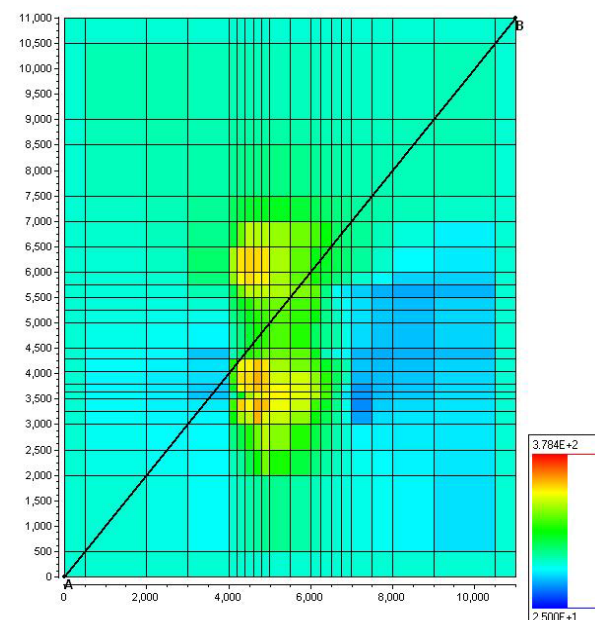
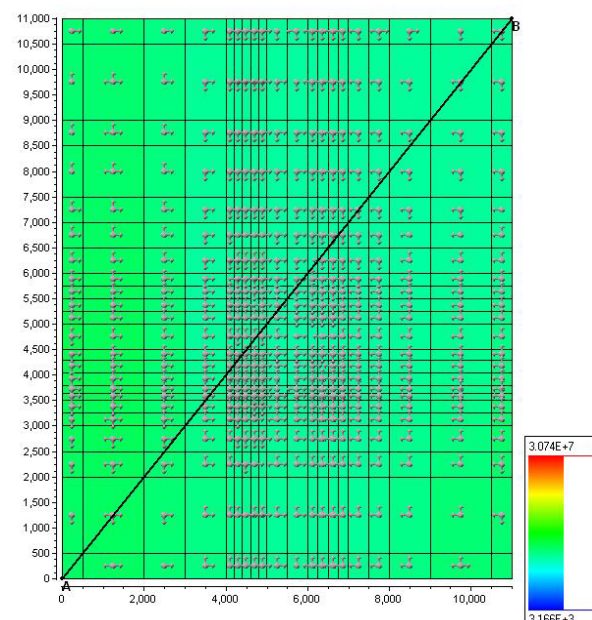
**Around 500 m a.s.l.**

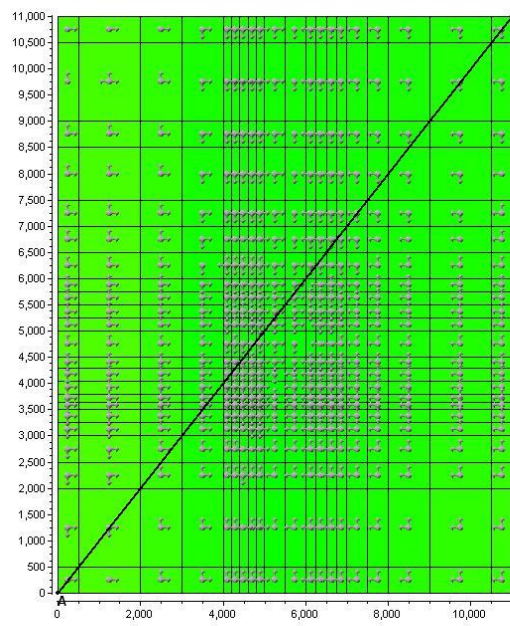
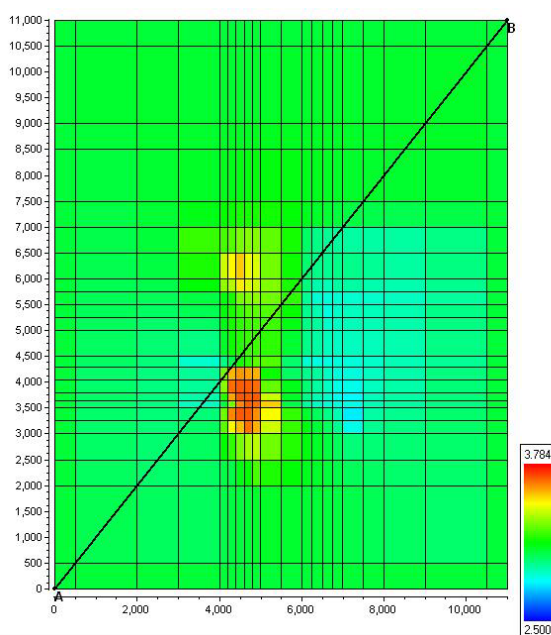
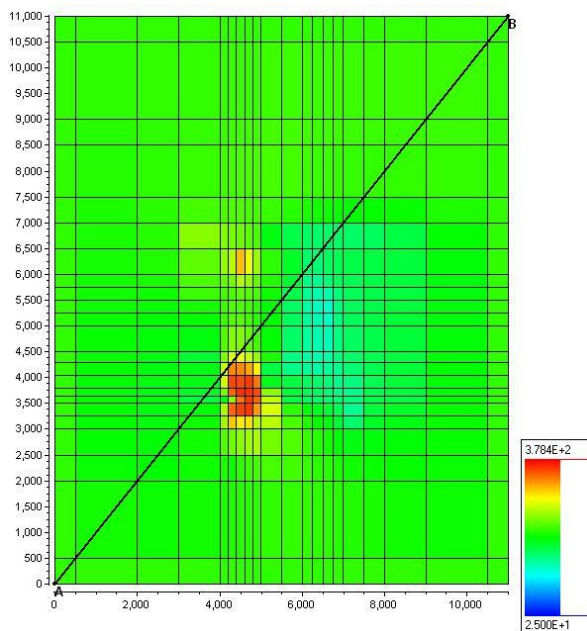
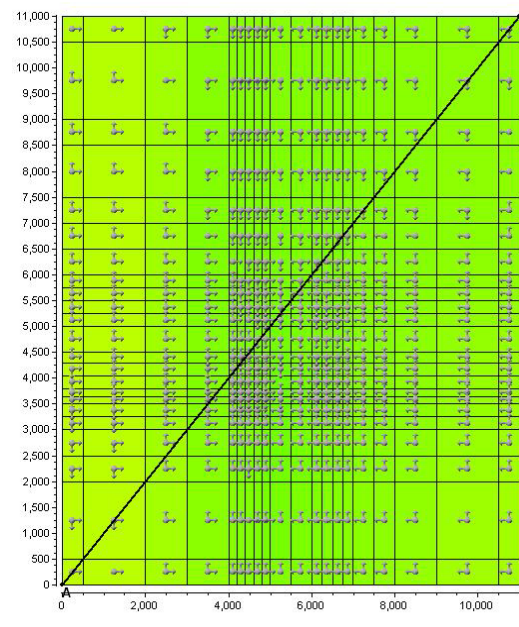


**Temperature**



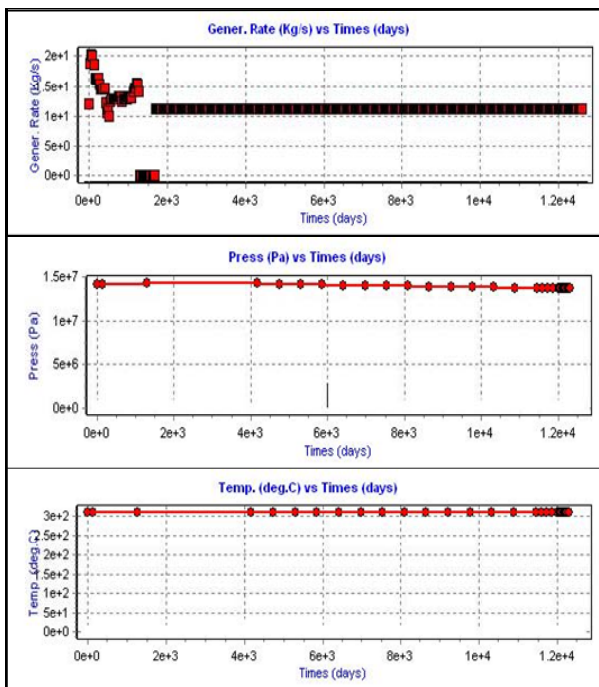
**Around 500 m b.s.l.**



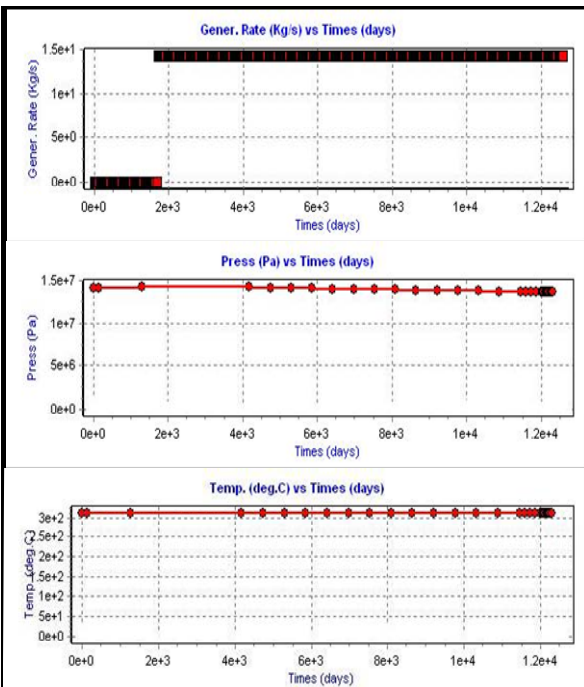
**Pressure****Around 1000 m b.s.l.****Temperature****Around 1500 m b.s.l.**

**APPENDIX IV: Calculated pressure and temperature profiles of wells  
in future forecast, between years 2001 and 2006**

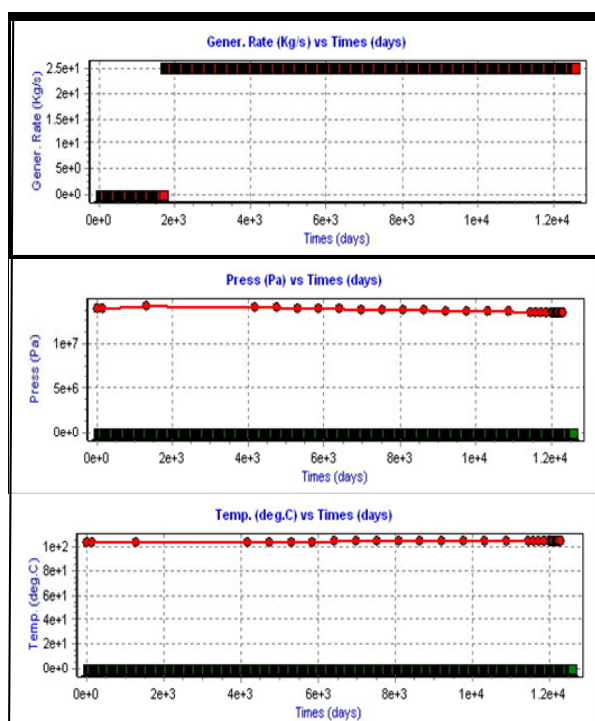
**Pad LHD-4 (well LHD-8)**

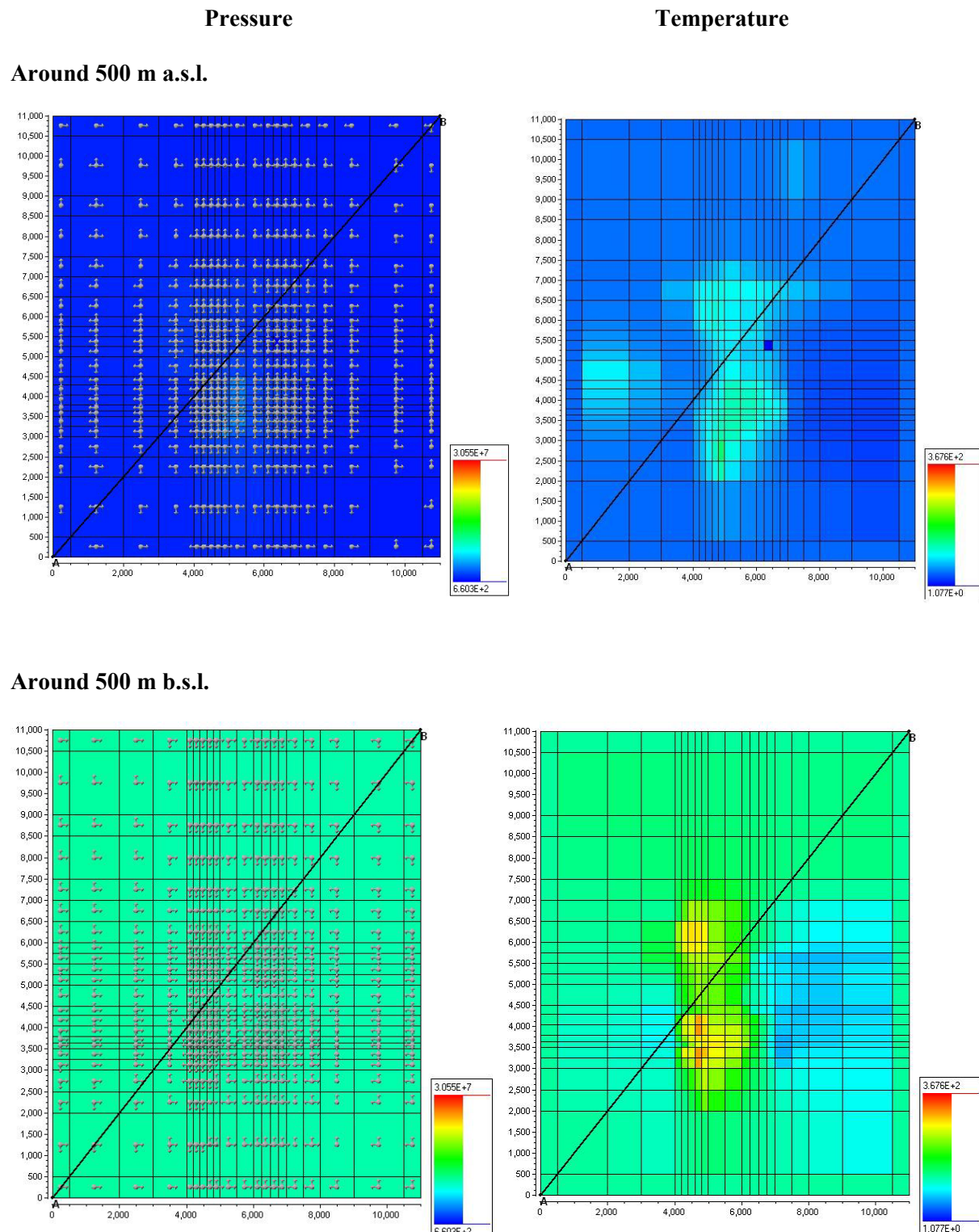


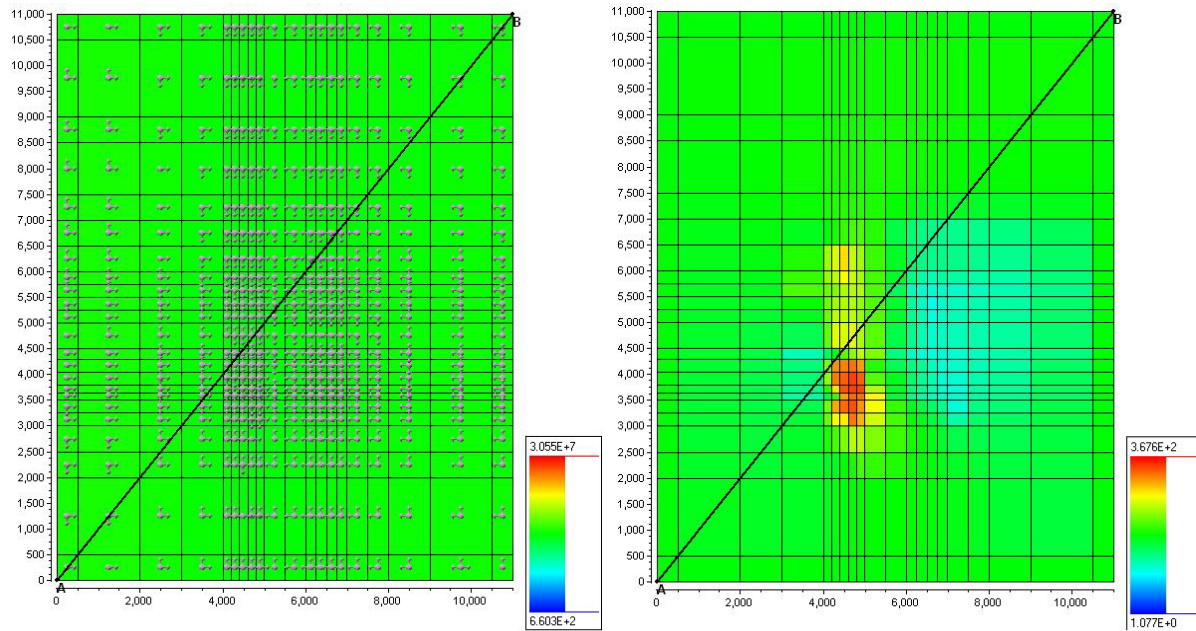
**Pad LHD-13 (well LHD-17)**



**Pad LHD-5 (well LHD-20)**



**APPENDIX V: Distribution of pressure and temperature in forecast at year 2036**


**Pressure****Temperature****Around 1000 m b.s.l.****Around 1500 m b.s.l.**